nature immunology

A gammaherpesvirus provides protection against allergic asthma by inducing the replacement of resident alveolar macrophages with regulatory monocytes

Bénédicte Machiels[1,7], Mickael Dourcy[1,7], Xue Xiao[1], Justine Javaux[1], Claire Mesnil[2], Catherine Sabatel[2], Daniel Desmecht[3], François Lallemand[4], Philippe Martinive[4], Hamida Hammad[5], Martin Guilliams[5], Benjamin Dewals[1], Alain Vanderplasschen[1], Bart N Lambrecht[5,6], Fabrice Bureau[2] & Laurent Gillet[1]

The hygiene hypothesis postulates that the recent increase in allergic diseases such as asthma and hay fever observed in Western countries is linked to reduced exposure to childhood infections. Here we investigated how infection with a gammaherpesvirus affected the subsequent development of allergic asthma. We found that murid herpesvirus 4 (MuHV-4) inhibited the development of house dust mite (HDM)-induced experimental asthma by modulating lung innate immune cells. Specifically, infection with MuHV-4 caused the replacement of resident alveolar macrophages (AMs) by monocytes with regulatory functions. Monocyte-derived AMs blocked the ability of dendritic cells to trigger a HDM-specific response by the T_H2 subset of helper T cells. Our results indicate that replacement of embryonic AMs by regulatory monocytes is a major mechanism underlying the long-term training of lung immunity after infection.

The immune system continuously faces environmental antigens and microorganisms that drive different forms of trained immunity[1–3]. While this training effect of prior microbial exposure is ignored in most animal models of disease, which are most often studied in specific pathogen-free conditions, normalizing environmental and microbial exposure can recapitulate adult human immunological traits in such animals[4–6].

Asthma is a major public health problem that affects 300 million people worldwide, among which are a large proportion of children[5]. The substantial increase in asthma prevalence observed in the Westernized world has occurred together with major changes in human exposure to microorganisms that cause chronic infections or that are part of a healthy and diverse microbiome[4]. The hygiene hypothesis proposes that the increase in allergic diseases in affluent countries is linked to reduced exposure to infections during early childhood, when there is a window of opportunity for becoming sensitized to allergens[7]. Early-life infection of children with Epstein-Barr virus (EBV) is suggested to protect the children against persistent sensitization to immunoglobulin E (IgE)[8,9]. The increased incidence of allergic asthma could therefore be associated in part with the increased age of seroconversion to EBV[10–12] or to other herpesviruses that is observed in developed countries.

The gammaherpesviruses EBV and Kaposi's sarcoma–associated herpesvirus are among the most prevalent human viruses[13]; they establish lifelong persistence that remains asymptomatic or is associated with only mild symptoms in immunocompetent people. However, as these infections occur during childhood, they might have substantial training effects on the host immune system that are relevant to understanding the allergy epidemic[14]. Accordingly, the closely related virus murid herpesvirus 4 (MuHV-4) has been shown to alter immunity to bacteria[15] and vaccines[16] and might reverse inherited immunodeficiency[17] in mice. Here we infected BALB/c and C57BL/6 mice with MuHV-4 to investigate how infection with this gammaherpesvirus affected the development of allergic asthma. We found that respiratory infection with MuHV-4 conferred strong and lasting protection against airway allergy through the replacement of resident alveolar macrophages (AMs) with recruited regulatory monocytes of bone marrow (BM) origin.

RESULTS

MuHV-4 infection inhibits HDM-induced allergic asthma

To address the effect of infection with a gammaherpesvirus on airway allergy, we infected 8-week-old female BALB/c mice intranasally, under general anesthesia, with 1×10^4 plaque-forming units (PFU) of MuHV-4. At 30 d after infection, a period that allows the establishment of latency[18] (**Fig. 1a**,**b**), mice received three consecutive instillations of house dust mite (HDM) at a dose of 100 µg, at 1-week intervals, and were euthanized 3 d later[19] (HDM high-dose model; **Supplementary Fig. 1a**). Mock-infected mice or MuHV-4-infected

[1]Immunology-Vaccinology, Department of Infectious and Parasitic Diseases, Faculty of Veterinary Medicine – FARAH, University of Liège, Liège, Belgium. [2]Cellular and Molecular Immunology, Department of Functional Sciences, Faculty of Veterinary Medicine – GIGA, University of Liège, Liège, Belgium. [3]Department of Pathology, Faculty of Veterinary Medicine – FARAH, University of Liège, Liège, Belgium. [4]Department of Radiology, University Hospital Liège, Liège, Belgium. [5]VIB Center for Inflammation Research, Ghent University, Ghent, Belgium. [6]Department of Pulmonary Medicine, Erasmus Medical Center, Rotterdam, the Netherlands. [7]These authors contributed equally to this work. Correspondence should be addressed to L.G. (l.gillet@ulg.ac.be).

Received 18 January; accepted 20 September; published online 16 October 2017; doi:10.1038/ni.3857

mice that received saline (NaCl) instead of HDM (mock NaCl mice or MuHV-4 NaCl mice, respectively) were used as controls. MuHV-4-infected mice exposed to HDM (MuHV-4 HDM mice) displayed reduced peribronchial and perivascular infiltration by inflammatory cells, a quasi-absence of goblet-cell hyperplasia (**Fig. 1c**), fewer eosinophils in broncho-alveolar lavage fluid (BALF) (**Fig. 1d**) and decreased concentrations of interleukin 4 (IL-4), IL-5, IL-13 and IL-6 in BALF (**Fig. 1e**), relative to that of mock-infected mice exposed to HDM (mock HDM mice). There was less proliferation, as well as less production of IL-5, IL-13, IL-6 and IL-10, by mediastinal lymph node (MLN) cells obtained from MuHV-4 HDM mice and stimulated *in vitro* with HDM than by similarly stimulated MLN cells from mock HDM mice (**Fig. 1f**,**g**). However, the number of lymphocytes in BALF and secretion of interferon-γ (IFN-γ) from MLN cells stimulated *in vitro* with HDM were comparable for mock HDM mice and MuHV-4 HDM mice (**Fig. 1d**,**g**), which indicated that infection with MuHV-4 impaired mainly a response by the T_H2 subset of helper T cells. In addition, in contrast to mock HDM mice, MuHV-4 HDM mice did not show an increase in serum IgE at euthanasia (**Fig. 1h**).

Infection with MuHV-4 also suppressed all the key features of asthma in 8-week-old female BALB/c and C57BL/6 mice exposed to a low dose (10 μg) of HDM, in contrast to results obtained for their mock-infected counterparts treated similarly (**Supplementary Fig. 1b–f**), which indicated that intranasal infection with MuHV-4 provided protection against HDM-induced asthma to mice on distinct genetic backgrounds. Finally, MuHV-4 HDM C57BL/6 mice displayed lower titers of HDM-specific IgE and IgG1 antibodies, but higher titers of HDM-specific IgG2c, than those of mock HDM C57BL/6 mice (**Supplementary Fig. 1g**); this showed that infection with MuHV-4 allowed an immune response to HDM and did not induce global anergy.

As the immunomodulatory effects of viruses can depend on the age of mice at the time of infection[20], we investigated the susceptibility of 3-week-old BALB/c mice to develop HDM-induced asthma following infection with MuHV-4. Similar to results obtained with adult mice, HDM-induced airway allergy was suppressed in MuHV-4-infected young mice at 1 month after infection (**Supplementary Fig. 2**). To investigate how protection against asthma was influenced by the schedule of HDM exposure following infection with MuHV-4, we

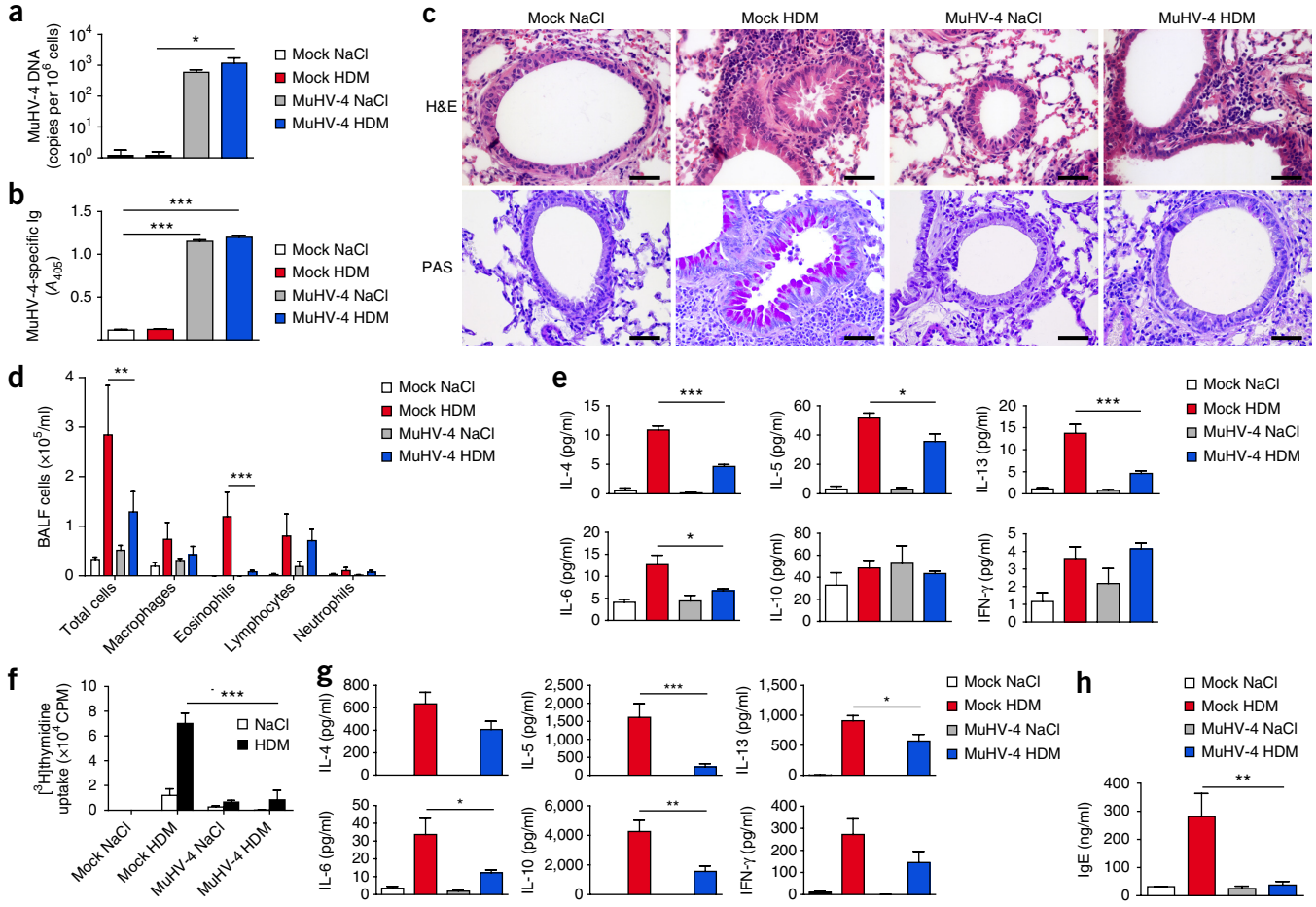

Figure 1 Infection with MuHV-4 inhibits the development of HDM-induced allergic asthma. (**a**) qPCR analysis of MuHV-4 genomic DNA in splenic cells from BALB/c mice (key) mock infected or infected with MuHV-4 intranasally and treated with the HDM high-dose model 30 d later (three sequential intranasal instillations of saline or 100 μg HDM at 7-day intervals and euthanasia 3 d after the final administration of saline or HDM; **Supplementary Fig. 1a**), assessed at death. (**b**–**e**,**h**) ELISA of MuHV-4-specific immunoglobulins (Ig) in serum (**b**), histological analysis of lung sections stained with hematoxylin and eosin (H&E) or periodic acid Schiff (PAS) (**c**), total and differential cell counts in BALF (**d**), ELISA of cytokines in BALF (**e**) and ELISA of total IgE in serum (**h**) from mice as in **a**. Results in **b** presented as absorbance at 405 nm (A_{405}). Scale bars (**c**), 100 μm. (**f**,**g**) Uptake of [^{3}H]thymidine into MLN cells (**f**) and ELISA of cytokines in supernatants of MLN cells (**g**) obtained from mice as in **a** and assessed without restimulation (**f** (NaCl in key)) or after restimulation for 3 d *ex vivo* with HDM (30 μg/ml) (**f** (key), **g**). CPM, counts per minute. $^*P < 0.05$, $^{**}P < 0.01$ and $^{***}P < 0.001$ (two-way analysis of variance (ANOVA) and Tukey's multiple-comparison test). Data are representative of at least three independent experiments with five mice per group (mean + s.e.m. in **a**,**b**,**d**–**h**).

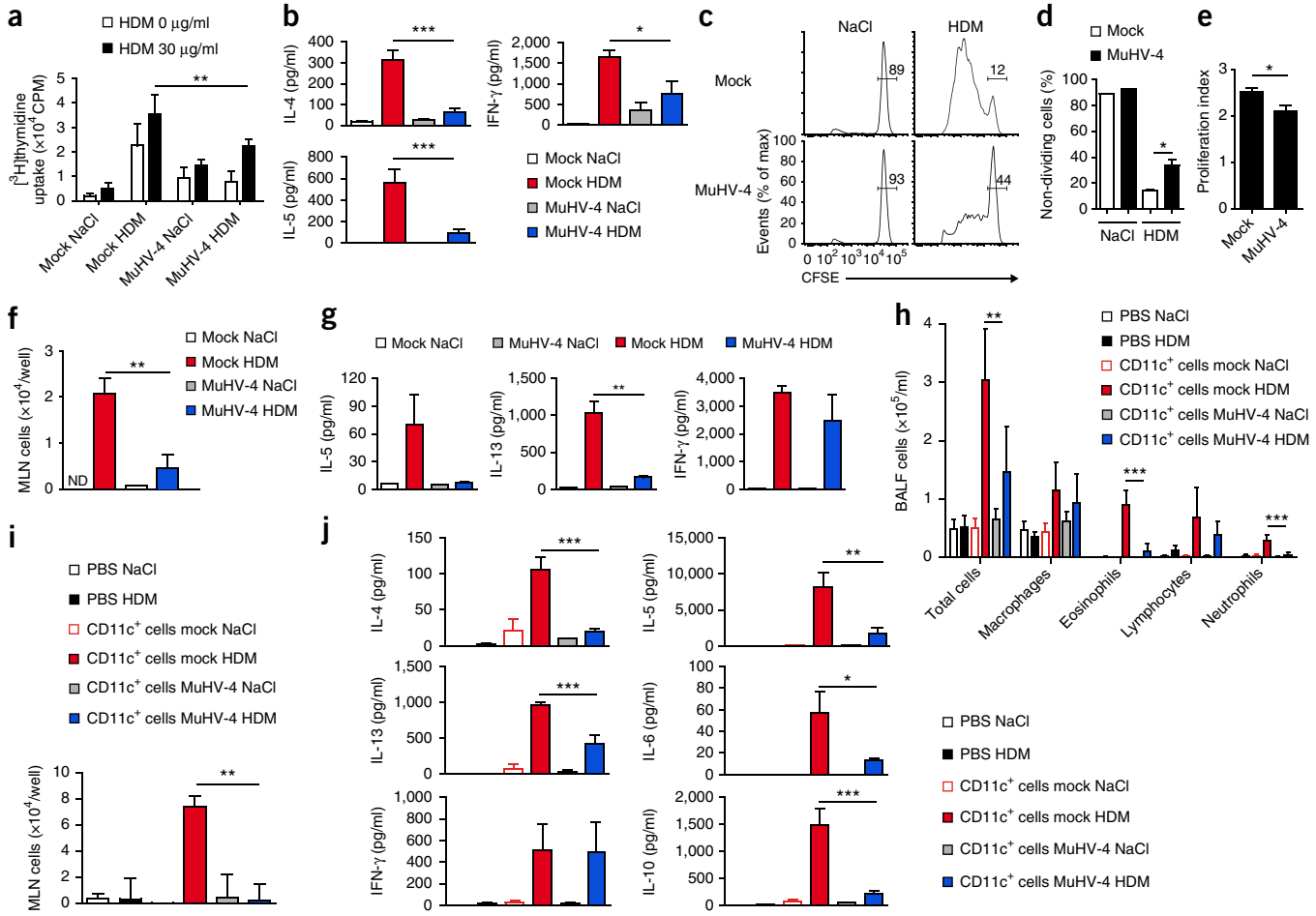

Figure 2 Infection with MuHV-4 affects the priming of HDM-induced T_H2 responses. (**a**,**b**) Uptake of [^{3}H]thymidine into MLN cells (**a**) and ELISA of cytokines in supernatants of MLN cells (**b**) from BALB/c mice mock infected or infected with MuHV-4 intranasally and sensitized 30 d after infection with saline or 100 μg HDM (horizontal axis), obtained at euthanasia 3 d later and assessed without restimulation (0 μg/ml; **a** (key)) or after restimulation for 3 d *ex vivo* with HDM (30 μg/ml) (**a** (key), **b**). (**c**,**d**) Flow-cytometry analysis of the *in vivo* population expansion of 1-DERβ T cells (assessed as CFSE dilution) (**c**) and frequency of non-dividing 1-DERβ T cells among MLN cells (**d**) in mock- or MuHV-4-infected C57BL/6 recipient mice given adoptive transfer of CFSE-labeled 1-DERβ T cells on day 30 after infection, along with saline or 10 μg HDM (simultaneously), assessed at euthanasia 3 d later. Numbers above bracketed lines (**c**) indicate percent non-divided (CFSE$^+$) cells. (**e**) Proliferation index of cells in HDM-sensitized mice as in **c**,**d** (calculated as total divisions divided by the number of cells that went into division). (**f**) Proliferation of total MLN cells obtained from mice as in **c**,**d** and restimulated *ex vivo* with HDM, presented as the abundance of those cells relative to that of their counterparts restimulated *ex vivo* with saline. ND, not detected. (**g**) ELISA of cytokines in supernatants of MLN cells obtained from mice as in **c**,**d** and restimulated for 3 d *ex vivo* with HDM. (**h**) Total and differential cell counts in BALF from recipient BALB/c mice given PBS or CD11c$^+$ cells purified from the MLNs of mock- or MuHV-4-infected BALB/c (sensitized for 3 d with HDM), followed by challenge of the host mice with saline or 10 μg HDM 9 d after cell transfer (key) and analysis at euthanasia 3 d later. (**i**) Proliferation of total MLN cells obtained from mice as in **h** and restimulated *ex vivo* with HDM (calculated as in **f**). (**j**) ELISA of cytokines in supernatants of MLN cells obtained from mice as in **h** and restimulated for 3 d *ex vivo* with HDM. $^*P < 0.05$, $^{**}P < 0.01$ and $^{***}P < 0.001$ (two-way ANOVA and Tukey's multiple-comparison test (**a**,**b**,**f**–**j**) or Student's *t*-test (**d**, **e**)). Data are representative of two independent experiments with five mice per group (mean + s.e.m. in **a**,**b**,**d**–**j**).

induced asthma in 8-week-old BALB/c mice with a high dose of HDM (100 μg) at 7, 30 or 60 d after infection. We observed a reduction in the features of asthma in all MuHV-4 HDM mice, relative to that of mock HDM mice (**Supplementary Fig. 3**). This indicated that the protection against asthma conferred by MuHV-4 was induced early after infection and was maintained over time.

MuHV-4 latency in mice involves production of IFN-γ that can trigger a heightened innate-immunity-activation state directed against subsequent heterologous infections[15]. To investigate whether MuHV-4 latency was required for protection against asthma, we assessed the development of HDM-induced asthma in 8-week-old BALB/c mice infected with wild-type MuHV-4, two latency-deficient MuHV-4 mutants (MuHV-4 FS73 and MuHV-4 Del73)[21] or the corresponding revertant (MuHV-4 Rev73)[21]. Infection with each of the four MuHV-4 strains, followed by treatment with HDM, induced attenuation of lung eosinophilia relative to that of mock HDM mice, as well as an absence of histological lesions (**Supplementary Fig. 4**). This showed that viral latency was not required for subsequent protection against asthma.

MuHV-4 infection affects the priming of HDM-induced T_H2 responses

We next assessed the effect of infection with MuHV-4 on the sensitization phase of asthma[5] in 8-week-old BALB/c mice exposed to a single instillation of HDM at 1 month after infection. MLN cells isolated from MuHV-4 HDM mice 3 d after HDM treatment showed less proliferation and secretion of IL-4 and IL-5 after restimulation

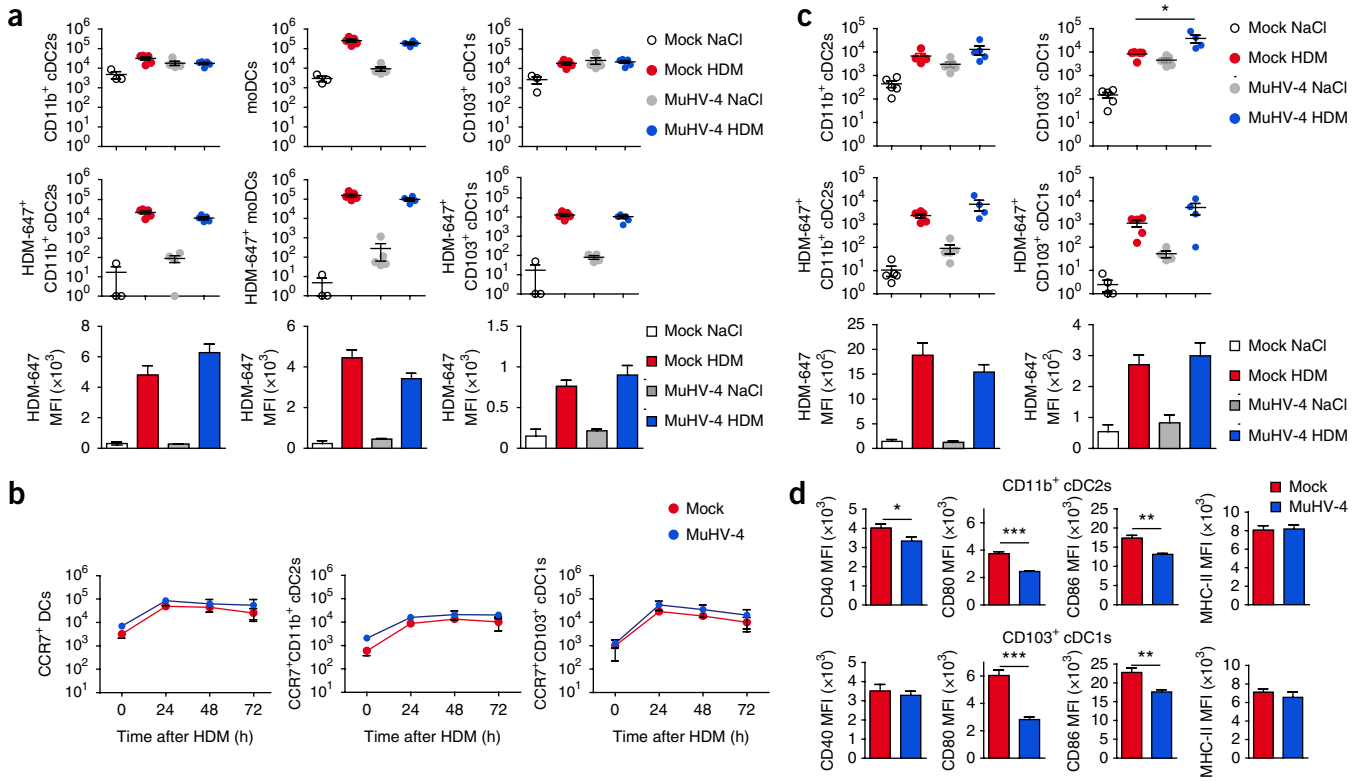

Figure 3 Infection with MuHV-4 affects the maturation of MLN DCs. (**a**) Absolute number (by flow cytometry) of total (top row) or HDM-647$^+$ (middle row) cDC2s (CD11b$^+$Ly6C$^-$CD64$^-$) (left), monocyte-derived DCs (moDCs: CD11b$^+$Ly6C^{int}CD64$^+$) (middle) or cDC1s (CD11b$^-$CD103$^+$) (right) in the lungs of BALB/c mice mock infected or infected with MuHV-4 intranasally and sensitized 30 d after infection with a single instillation of saline or 100 μg HDM-647, then euthanized 24 h later (top and middle rows), and mean fluorescence intensity (MFI) of Alexa Fluor 647 in the cells above (bottom row). (**b**) Absolute number (by flow cytometry) of total migratory CCR7$^+$ DCs (live, SiglecF$^-$Ly6G$^-$Ly6C$^-$CD64$^-$CD3$^-$CD19$^-$CD11c$^+$MHCII^{hi}CCR7$^+$) (left), cDC1s (middle) and cDC2s (right) in the MLNs of BALB/c mice mock infected or infected with MuHV-4 intranasally and treated 30 d after infection with a single instillation of 100 μg HDM, then euthanized immediately (without sensitization; 0 h) or at 24, 48 and 72 h after such sensitization. (**c**) Absolute number (by flow cytometry) of total and HDM-647$^+$ DCs (gated as in **b**) in the MLNs of BALB/c mice infected and sensitized as in **a**, then euthanized 72 h later (top and middle), and MFI of Alexa Fluor 647 in the cells above (bottom). (**d**) MFI (assessed by flow cytometry) of the staining of CD40, CD80, CD86 and MHC class II on migratory CCR7$^+$ DCs (strategy, **Supplementary Fig. 5**) from the MLNs of BALB/c mice infected and sensitized as in **b**, then euthanized 48 h later. Each symbol (**a**,**c**) represents an individual mouse; small horizontal lines indicate the mean (± s.e.m.). $^*P < 0.05$, $^{**}P < 0.01$ and $^{***}P < 0.001$ (two-way ANOVA and Tukey's multiple-comparison test (**a**–**c**) or Student's *t*-test (**d**)). Data are representative of two independent experiments with three mice (mock NaCl) or five mice per group (other conditions) (mean + s.e.m.).

ex vivo than that of MLN cells obtained from mock HDM mice and restimulated similarly *ex vivo* (**Fig. 2a**,**b**). To further explore the effect of infection with MuHV-4 on the HDM-specific T cell response, we used 1-DerβTg mice, which transgenically express a T cell antigen receptor that recognizes an immunodominant peptide from the HDM-derived allergen Derp-1 (ref. 22). We labeled 1-DerβTg splenic CD4$^+$ T cells with the division-tracking dye CFSE and adoptively transferred the cells into mock- or MuHV-4-infected host mice 1 month after infection, then sensitized the host mice with a single dose of HDM (10 μg). At 4 d after sensitization, 1-DerβTg CD4$^+$ T cells showed less proliferation in MuHV-4 HDM mice than in mock HDM mice (**Fig. 2c**–**e**). Furthermore, total MLN cells from MuHV-4 HDM mice proliferated less and produced less IL-5 and IL-13 after restimulation *ex vivo* than did MLN cells isolated from mock HDM mice and restimulated similarly *ex vivo*, while IFN-γ production in the two groups was comparable (**Fig. 2f**,**g**). This indicated that infection with MuHV-4 impaired the T_H2 polarization of HDM-specific T cells but seemed to not affect the T_H1 polarization of the immune response.

Dendritic cells (DCs) are necessary and sufficient to induce T_H2 sensitization against lung allergens[23]. To investigate the ability of DCs to initiate an HDM-specific T_H2 response following infection with MuHV-4, we sensitized mock- or MuHV-4-infected mice with a single dose of HDM (100 μg) or not, and, 3 d later, transferred CD11c$^+$ MLN cells from those mice into naive 8-week-old female BALB/c host mice. At 9 d after cell transfer, recipient mice were challenged with a single dose of HDM (10 μg) or saline and were euthanized 3 d later. While eosinophilic infiltration was not observed in the lungs of mice given transfer of CD11c$^+$ MLN cells from mock NaCl mice, substantial lung eosinophilia was present in mice given transfer of CD11c$^+$ MLN cells from mock HDM mice (**Fig. 2h**). In contrast, eosinophilic infiltration was not observed in the lungs of mice given transfer of MLN CD11c$^+$ cells from MuHV-4 HDM mice (**Fig. 2h**). In addition, restimulation *ex vivo* with HDM induced less proliferation and less production of IL-4, IL-5 and IL-13 by MLN cells from mice given transfer of CD11c$^+$ DCs from MuHV-4 HDM donors than by such cells from mice given transfer of CD11c$^+$ DCs from mock HDM donors, while IFN-γ production was similar in these two experimental conditions (**Fig. 2i**,**j**). Notably, transfer of CD11c$^+$ DCs from MuHV-4 HDM mice did not transfer infection (data not shown). These results indicated that infection with MuHV-4 blocked the ability of DCs to induce T_H2 effector responses to HDM *in vivo*.

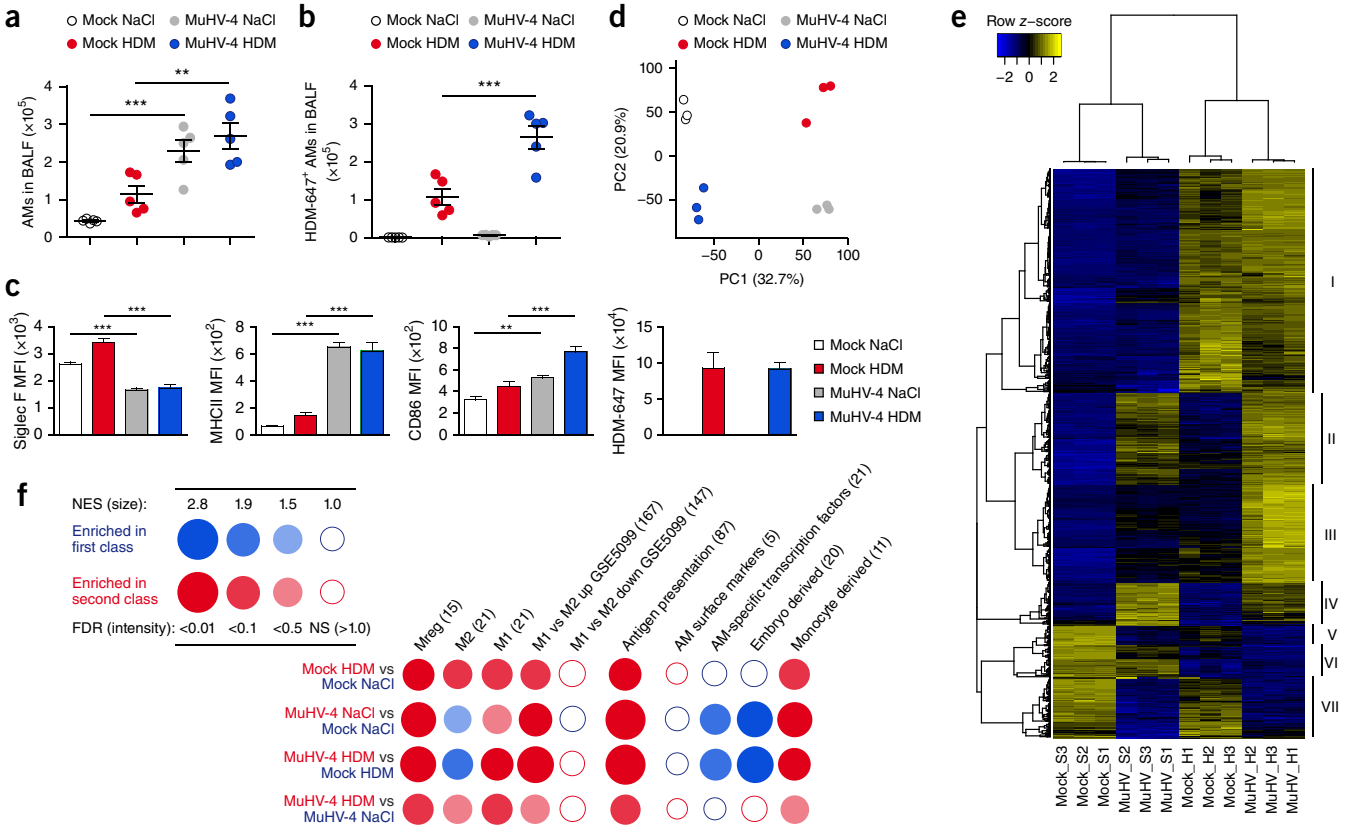

Figure 4 Infection with MuHV-4 affects the phenotype of AMs. (**a**–**c**) Absolute number (by flow cytometry) of total AMs (**a**) and HDM-647$^+$ AMs (**b**) and MFI of SiglecF, MHC class II, CD86 and HDM-647 on AMs (**c**) isolated from BALF of BALB/c mice mock infected or infected with MuHV-4 intranasally and sensitized with a single instillation of saline or 100 μg HDM-647 (key), then euthanized 24 h later. (**d**–**f**) Transcriptomics analysis of AMs isolated from BALF of BALB/c mice ($n = 6$ per group) mock infected or infected with MuHV-4 intranasally and sensitized with a single instillation of saline 100 μg HDM, assessed by principal-component analysis (including the proportion of the variability explained (in parentheses) by principal component 1 (PC1) or principal component 2 (PC2)) (**d**), expression (key) of all genes expressed differentially ($P < 1 \times 10^{-5}$; change in expression of over twofold) in each pairwise comparison (of all four groups, two by two; S, saline; H, HDM; 1–3, one to three biological replicates, with two mice per replicate) (**e**) or enrichment for transcriptomic fingerprints (gene sets) specific for polarization as M1 or M2 macrophage or genes encoding regulatory molecules (Mreg), as well as for the gene sets GSE5099_CLASSICAL_M1_VS_ALTERNATIVE_M2_MACROPHAGE_UP and GSE5099_CLASSICAL_M1_VS_ALTERNATIVE_M2_MACROPHAGE_DN (GEO database) and mmu04612 (KEGG database), by gene-set–enrichment analysis with BubbleGUM software (**f**); brackets along top and left margins (**e**) indicate hierarchical clustering, and I–VII along right margin (**e**) indicate clusters; in **f** (key at top), color indicates cell subset showing enrichment for the gene set, and size of symbol and color intensity indicate significance of enrichment (surface area proportional to absolute value of the normalized enrichment score (NES); color intensity indicates the false-discovery rate (FDR)). Numbers in parentheses (above) indicate number of genes. NS, not significant. Each symbol (**a**,**b**,**d**) represents an individual mouse; small horizontal lines (**a**,**b**) indicate the mean (± s.e.m.). *$P < 0.05$, **$P < 0.01$ and ***$P < 0.001$ (two-way ANOVA and Tukey's multiple-comparison test (**a**–**c**)). Data are representative of at least three independent experiments with five mice per group (mean + s.e.m. in **c**).

MuHV-4 infection affects the maturation of MLN DCs

Lungs contain subtypes of DCs categorized as plasmacytoid DCs, monocyte-derived DCs and conventional DCs (cDCs)[24], further separated into the CD103$^+$ cDC1 and CD11b$^+$ cDC2 subsets[25]. cDCs and monocyte-derived DCs contribute to HDM-induced airway allergy, with lung CD11b$^+$ cDC2s being necessary and sufficient to induce allergic sensitization[22,26]. We assessed the effect of infection with MuHV-4 on the ability of cDCs and monocyte-derived DCs to take up HDM, transport it to the MLNs and express maturation markers. Mock- and MuHV-4-infected 8-week-old female BALB/c mice were sensitized with 100 μg of Alexa Fluor 647–conjugated HDM (HDM-647), and the ability of those subsets (cDC1, cDC2 and monocyte-derived DC) of lung DCs (live, CD45$^+$, non-autofluorescent, SiglecF$^-$Ly6G$^-$CD3$^-$CD19$^-$CD11c$^+$MHCII$^+$ cells) to internalize HDM and to migrate to the MLNs was analyzed by flow cytometry 1 d later. Antigen uptake by CD103$^+$ cDC1s, CD11b$^+$ cDC2s and monocyte-derived DCs was similar in mock HDM mice and MuHV-4 HDM mice (**Fig. 3a**). At 24, 48 and 72 h after treatment with HDM, migratory CCR7^{hi} cells in the MLNs were mainly CD11b$^+$ cDC2s and CD103$^+$ cDC1s in mock HDM mice and MuHV-4 HDM mice (**Fig. 3b**). At 72 h after treatment with HDM, the number of HDM-647$^+$ CD103$^+$ cDC1s and CD11b$^+$ cDC2s in the MLNs of MuHV-4 HDM mice was similar to that in the MLNs of mock HDM mice (**Fig. 3c**). At 2 d after sensitization with HDM, we saw lower expression of the DC maturation markers CD40, CD80 and CD86 in CCR7^{hi}CD11b$^+$ cDC2s from MuHV-4 HDM mice than in those from mock HDM mice, while expression of major histocompatibility complex (MHC) class II in these two groups was similar (**Fig. 3d** and **Supplementary Fig. 5**). This indicated that infection with MuHV-4 did not block the uptake of HDM and its transport to MLNs by DCs, but it did reduce the expression of costimulatory molecules by migratory DCs.

MuHV-4 infection affects AM phenotype

To determine whether the effect of infection with MuHV-4 on resident cDCs was due to systemic factors or local factors, we compared

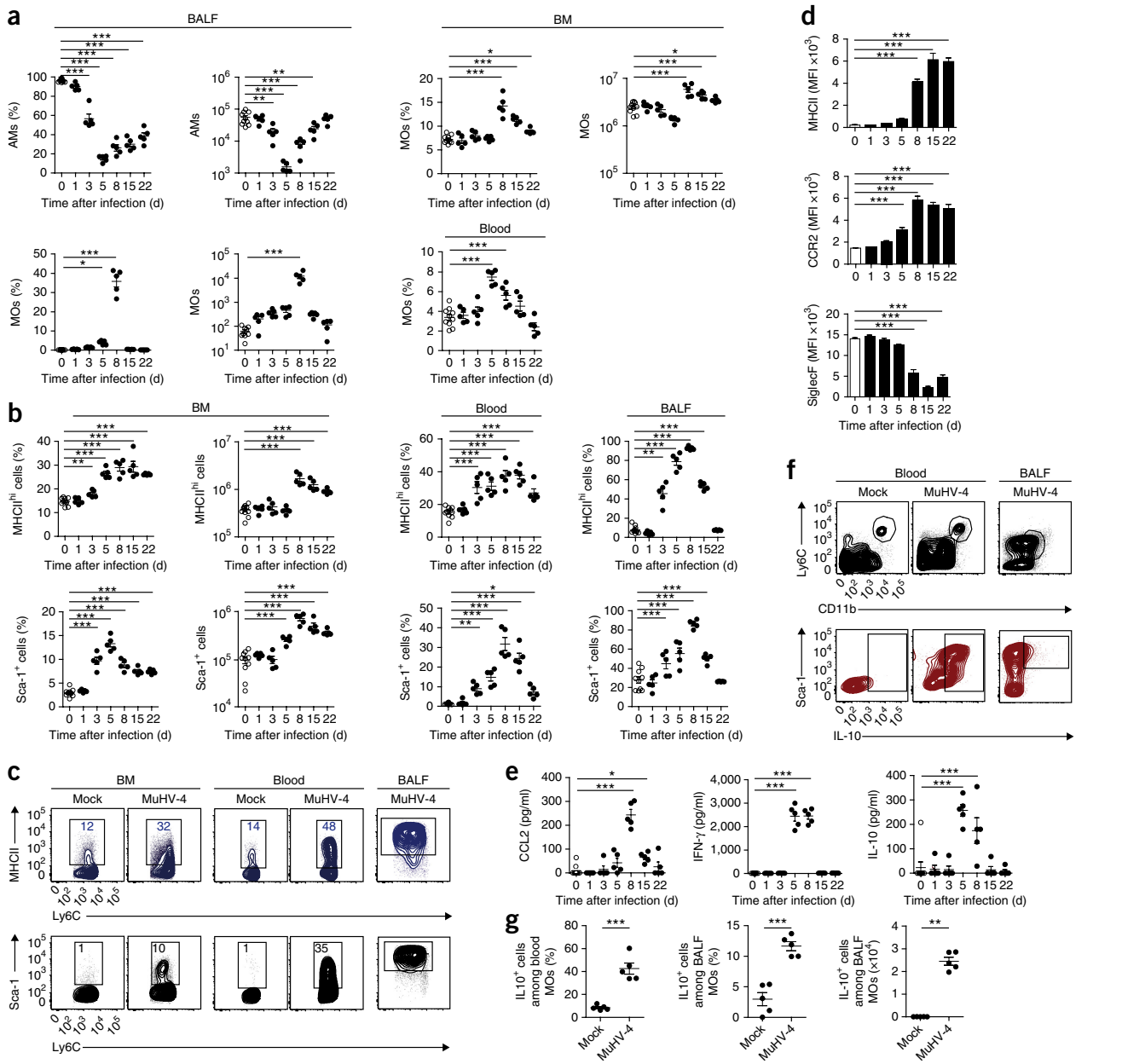

Figure 5 MuHV4 induces the replacement of resident AMs by regulatory monocytes. (**a**,**b**) Frequency and absolute number (by flow cytometry) of AMs (live, CD11c$^+$, autofluorescent cells) in BALF and Ly6C^{hi} monocytes (MOs) in BALF (live, CD11c$^-$, non-autofluorescent, CD19$^-$Ly6G$^-$SiglecF$^-$CD11b$^+$CCR2$^+$Ly6C^{hi} cells), BM (live, CD19$^-$Ly6G$^-$SiglecF$^-$CD11b$^+$Ly6C^{hi} cells) and blood (live, CD19$^-$Ly6G$^-$SiglecF$^-$CD11b$^+$Ly6C^{hi} cells) (gated as described in **Supplementary Fig. 8**) (**a**), and frequency and absolute number of MHCII^{hi} (top row) or Sca-1$^+$ (bottom row) Ly6C^{hi} monocytes (gated as in **a**) isolated from the BM, blood and BALF (**b**) BALB/c mice mock infected (day 0) or infected with MuHV-4 and euthanized at various times after infection (horizontal axes). (**c**) Flow cytometry of cells from the BM, blood and BALF (above plots) of BALB/c mice mock infected or at day 8 after infection with MuHV-4 (above plots), pre-gated on Ly6C^{hi} monocytes. Numbers in outlined areas indicate percent MHCII$^+$Ly6C^{hi} cells (top row) or Sca-1$^+$Ly6C^{hi} cells (bottom row). (**d**) MFI of MHC class II, CCR2 and SiglecF on AMs (**d**) and ELISA of CCL2, IFN-γ and IL-10 in BALF (**e**) at various times after infection as in **a**,**b** (horizontal axis). (**f**) Flow cytometry of Ly6C^{hi} monocytes in the blood and BALF (gated as in **a**) of BALB/c mice mock infected or at day 8 after infection with MuHV-4. Outlined areas indicate MHCII$^+$CD11b$^+$ monocytes (top row) or Sca-1$^+$IL-10^{hi} cells (bottom row). (**g**) Frequency and absolute number of IL-10-secreting cells among cells as in **f**. Each symbol (**a**,**b**,**e**,**g**) represents an individual mouse; small horizontal lines indicate the mean (± s.e.m.). $*P < 0.05$, $**P < 0.01$ and $***P < 0.001$ (one-way ANOVA and Dunnett's multiple-comparison test (**a**,**b**,**d**,**e**) or Student's *t*-test (**g**)). Data are representative of at least two independent experiments with ten mice per group (day 0) or five mice per group (other conditions) (mean + s.e.m. in **d**).

the effect of intranasal infection with MuHV-4 on HDM-induced asthma with that of intraperitoneal infection. Only intranasal infection protected mice against airway allergy (**Supplementary Fig. 6**). This indicated that pulmonary infection with MuHV-4 was needed to induce protection against asthma.

Airway-resident cDC are short-lived[27]. Among the cells that act together to shape lung T_H2 or tolerogenic responses[4], AMs are long-lived, represent the most abundant airway subset exposed to inhaled air and particles[28] and regulate the activation and antigen-presenting ability of DCs[29–31]. MuHV-4 virions infect AMs after intranasal infection[32].

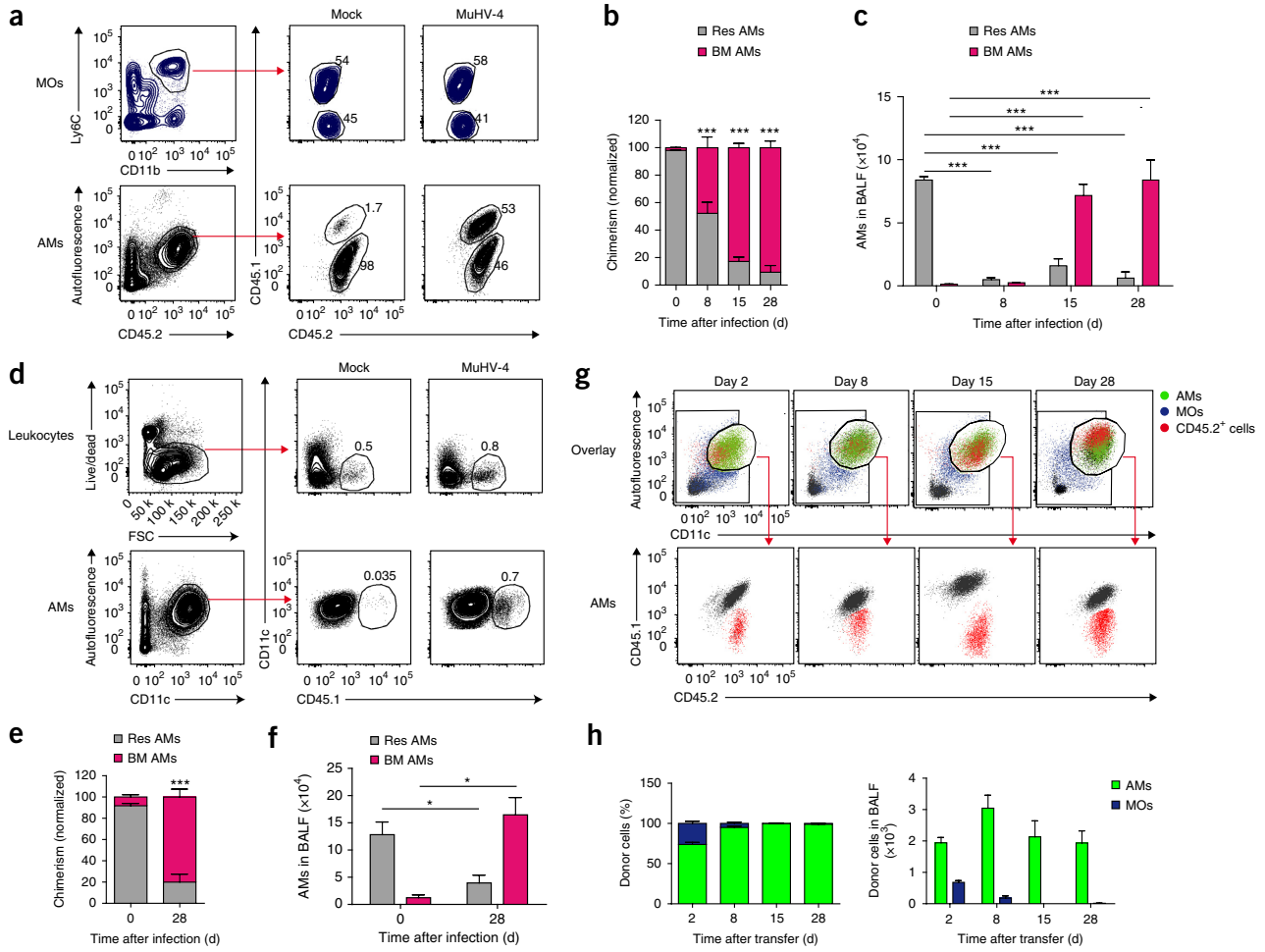

Figure 6 Monocyte-derived AMs persist long term in MuHV-4-infected mice. (**a**) Flow cytometry to assess the chimerism (staining of CD45.1 and CD45.2; middle and right) of blood monocytes and AMs (gated as at left, as defined in **Fig. 5a**) isolated from CD45.2$^+$ BALB/c recipient mice treated with partial-body irradiation (preserving the thorax) and given intravenous transfer of CD45.1$^+$CD45.2$^+$ BM cells, then mock infected or infected with MuHV-4 intranasally (above plots) 7 weeks after cell transfer and euthanized at day 28 after infection. Numbers adjacent to outlined areas (middle and right) indicate percent CD45.1$^+$CD45.2$^+$ (donor) cells (top area) or CD45.1$^-$CD45.2$^+$ (host) cells (bottom area). (**b**) Chimerism of resident (CD45.2$^+$) cells (Res AMs) and recruited (CD45.1$^+$CD45.2$^+$) cells (BM AMs) in AM populations of mice as in **a**, assessed at euthanasia at various times after infection (horizontal axis); results normalized to the chimerism of blood monocytes. (**c**) Total AMs of resident or BM origin (key) in BALF of mice as in **a**, assessed at euthanasia at various times after infection (horizontal axis). (**d**) Flow cytometry to assess the chimerism (staining of CD45.1; middle and right) of blood leukocytes and AMs (gated as at left, as defined in **Fig. 5a**) isolated from CD45.2$^+$ BALB/c non-irradiated recipient mice given intraperitoneal injection of 8×10^6 CD45.1$^+$ BM cells on their 11th day of life and mock infected or infected with MuHV-4 intranasally 7 weeks after cell transfer (above plots), then euthanized at day 28 after infection. Numbers adjacent to outlined areas indicate percent CD11c$^+$CD45.1$^+$ cells. (**e**,**f**) Chimerism of resident and recruited cells (as in **b**) (**e**) and total AMs of resident or BM origin in BALF (as in **c**) (**f**) of mice as in **d** at day 0 or 28 after infection (horizontal axes). (**g**) Flow-cytometry overlays of AMs, monocytes (gated as described in **Supplementary Fig. 8**) and transferred (CD45.2$^+$) cells (key) in BALF from BALB/c CD45.1$^+$ recipient mice infected intranasally with MuHV-4 and, at day 8 after infection, given intranasal transfer of 2×10^5 BM monocytes (live, CD19$^-$Ly6G$^-$SiglecF$^-$CD11b$^+$Ly6C^{hi} cells) sorted from donor CD45.2$^+$ BALB/c mice infected intranasally for 5 d with MuHV-4, assessed at various times after cell transfer (above plots). (**h**) Frequency of AMs and monocytes (key) among the CD45.2$^+$ population (top) and total CD45.2$^+$ AMs or monocytes (key) in BALF of mice as in **g** at various times after cell transfer (horizontal axes). $^*P < 0.05$ and $^{***}P < 0.001$, versus day 0 (one-way ANOVA and Dunnett's multiple-comparison test (**b**,**c**) or Student's *t*-test (**e**,**f**)). Data are representative of two experiments (**a**–**c**; mean + s.e.m. of $n = 5$ mice per time point (infected) or $n = 8$ mice (mock infected: $n = 1$ (days 0, 8 and 15) and $n = 5$ (day 28)) in **b**,**c**), two experiments (**d**–**f**; mean + s.e.m. of $n = 5$ mice per group in **e**,**f**) or two experiments (**g**,**h**; mean + s.e.m. in **h** of $n = 5$ mice per group).

We sensitized mock- and MuHV-4-infected mice with HDM-647 and compared the ability of their AMs (defined as live, CD11c$^+$, autofluorescent cells) to internalize allergens and to express critical activation markers. At 24 h after treatment with HDM, the number of total and HDM-647$^+$ AMs was greater in the MuHV-4 HDM mice than in the mock HDM mice (**Fig. 4a**,**b**). Simultaneously, we observed lower expression of SiglecF and higher expression of MHC class II and CD86 in MuHV-4 HDM AMs than in mock HDM AMs, while the ability to internalize HDM was similar for both groups (**Fig. 4c**).

Next we performed transcriptomics analysis of AMs from the BALF of mock- or MuHV-4-infected 8-week-old female BALB/c mice at 24 h after a single administration of HDM or saline (**Supplementary Fig. 7**). Principal-component analysis indicated that AMs from the four groups exhibited different gene-expression profiles (**Fig. 4d**). We identified genes induced by HDM (cluster I), by MuHV-4 (clusters II and IV) or by MuHV-4 and HDM together (cluster III), while the expression of some genes was reduced by infection with MuHV-4 (clusters V and VII) or by HDM (cluster VI), relative to their expression

by AMs from the mock NaCl group (**Fig. 4e**). Analysis of phenotypic molecular signatures with BubbleGUM, a tool that allows gene-set–enrichment analysis of transcriptomics data[33], revealed that infection with MuHV-4 induced a shift toward higher expression of genes encoding regulatory molecules or genes encoding products that reflect classical macrophage activation (M1), relative to the expression of genes encoding products that reflect alternative activation (M2) (**Fig. 4f** and **Supplementary Tables 1** and **2**). It also indicated that infection with MuHV-4 induced the upregulation of a large number of genes encoding products involved in antigen presentation, including genes encoding MHC class II molecules, and reduced expression of SiglecF (**Fig. 4f** and **Supplementary Tables 1** and **2**). Precursor cells of embryonic or postnatal origin can both durably colonize the alveolar niche to give rise to AMs[34]. BubbleGUM analysis of gene sets specific to an embryonic or postnatal origin of AMs[35] indicated that infection with MuHV-4 induced substantially higher expression of genes indicative of a monocytic origin relative to the expression of such genes in AMs from mock-infected mice (**Fig. 4f**).

Resident AMs are replaced by regulatory monocytes

To further investigate the outcome of respiratory infection with MuHV-4 on AMs, we used flow cytometry to characterize the AMs in BALF and to monitor the trafficking of monocytes from the BM to the lungs at 1, 3, 5, 8, 15 and 22 d after infection of 8-week-old female BALB/c mice with 1×10^4 PFU of MuHV-4. The number of AMs in the BALF of MuHV-4-infected mice at day 5 after infection was less than 20% that in the BALF of mock-infected mice (represented by day 0), then was progressively restored until day 22 (**Fig. 5a** and **Supplementary Fig. 8**). The disappearance of AMs observed in MuHV-4-infected mice was due to cell death, as revealed by staining with the apoptosis marker annexin V and the membrane-impermeable DNA-intercalating dye 7AAD (**Supplementary Fig. 8f**). From day 8 after infection, AMs from MuHV-4-infected mice had lower expression of SiglecF and higher expression of MHC class II and the chemokine receptor CCR2 than that of AMs from mock-infected mice (**Fig. 5d** and **Supplementary Fig. 8d**).

Massive recruitment into the alveolar space of CD19$^-$Ly6G$^-$SiglecF$^-$CD11b$^+$CCR2$^+$Ly6C^{hi} monocytes (which reached ~35% of all cells present in this location) was detected in MuHV-4-infected mice at day 8 after infection but was absent in the mock-infected group (**Fig. 5a**). We also observed a greater number of CD19$^-$Ly6G$^-$SiglecF$^-$CD11b$^+$Ly6C^{hi} monocytes (gated as described in **Supplementary Fig. 8**) in the blood and BM of MuHV-4-infected mice at day 5 after infection than in that of mock-infected mice (**Fig. 5a**). Increased expression of the lineage marker Sca-1 and MHC class II is associated with the acquisition of a regulatory profile in monocytes[36]. CD19$^-$Ly6G$^-$SiglecF$^-$CD11b$^+$CCR2$^+$Ly6C^{hi} monocytes in the BM, blood and BALF of MuHV-4-infected mice showed higher expression of Sca-1 and MHC class II from day 3 after infection, relative to that of such cells from mock-infected mice (**Fig. 5b**,**c**). These phenotypic changes persisted up to day 22 after infection in BM and blood (**Fig. 5b**,**c**), suggestive of a long-term effect on monocytes.

At steady state, BM-derived monocytes can efficiently colonize the alveolar niche if space is available[37] and generate long-lived, self-maintaining AMs that show minimal differences in gene-expression profile relative to that of embryo-derived resident AMs. We investigated whether BM-derived monocytes colonized the alveolar niche during the course of infection with MuHV-4. The emigration of CCR2$^+$ monocytes from the BM during infection is driven mainly by the chemokine CCL2 (ref. 38). We observed more CCL2 in the BALF of 8-week-old female BALB/c mice infected intranasally with

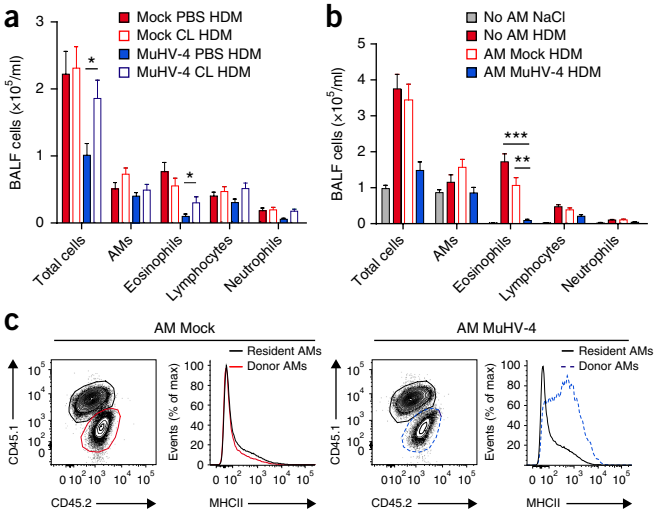

Figure 7 AMs from MuHV-4-infected mice are necessary and sufficient for blocking HDM-induced airway allergy. (**a**) Total and differential cell counts in BALF from BALB/c mice mock infected or infected with MuHV-4 intranasally, treated intranasally 30 d after infection with endotoxin-free PBS or liposomes containing clodronate (CL) and treated with the HDM high-dose model 2 weeks after clodronate treatment, assessed at euthanasia. (**b**) Total and differential cell counts in BALF from mock-infected CD45.1$^+$ recipient BALB/c mice given no AMs or intranasal transfer of AMs purified from the BALF of CD45.2$^+$ donor mice mock infected or infected (for 30 d) with MuHV-4 intranasally, followed by treatment of the host mice with the HDM high-dose model 3 d after cell transfer (key) and analysis at euthanasia. (**c**) Expression of MHC class II (right plot of pair) by resident and transferred (donor) AMs (gated as in left plot of pair) in host mice given AMs from donor mice as in **b**. $^*P < 0.05$, $^{**}P < 0.01$ and $^{***}P < 0.001$ (Student's *t*-test (**a**) or two-way ANOVA and Tukey's multiple-comparison test (**b**)). Data are representative of two independent experiments with five mice per group (mean + s.e.m. in **a**,**b**).

MuHV-4, at days 8 and 15 after infection, than in that of their mock-infected counterparts (**Fig. 5e**), along with more IFN-γ in serum (data not shown) and BALF (**Fig. 5e**), and more IL-10 in BALF at days 5 and 8 after infection (**Fig. 5e**). Moreover, detection of IL-10-secreting cells by flow cytometry showed that Ly6C^{hi}MHCII^{hi}Sca-1$^+$ blood and BAL monocytes from MuHV-4-infected mice produced more IL-10 than did those from mock-infected mice (**Fig. 5f**,**g**). These results showed that infection with MuHV-4 induced the death of resident embryonic AMs and the recruitment of BM-derived monocytes with regulatory properties.

Monocyte-derived AMs persist long term in MuHV-4-infected mice

We next investigated the origin of the AMs that occupied the alveolar niche at various times after infection. The engraftment of BM cells into lethally irradiated mice results in the replacement of most resident macrophages by cells from the transplanted BM. We engrafted donor total BM cells into irradiated recipient mice in which lung-resident AMs were protected from direct irradiation exposure by preservation of the thorax. Mice were infected intranasally with MuHV-4 at 7 weeks after BM transfer. At 0, 8, 15 and 28 d after infection, we observed partial chimerism among peripheral blood monocytes in both mock-infected mice and MuHV-4-infected mice, with 50–65% of blood CD19$^-$Ly6G$^-$SiglecF$^-$CD11b$^+$Ly6C^{hi} monocytes being of donor origin (**Fig. 6a**). Only 2% of lung AMs were of donor origin in mock-infected mice (**Fig. 6a**), which indicated minimal replacement of lung-resident AMs under these conditions, while donor chimerism

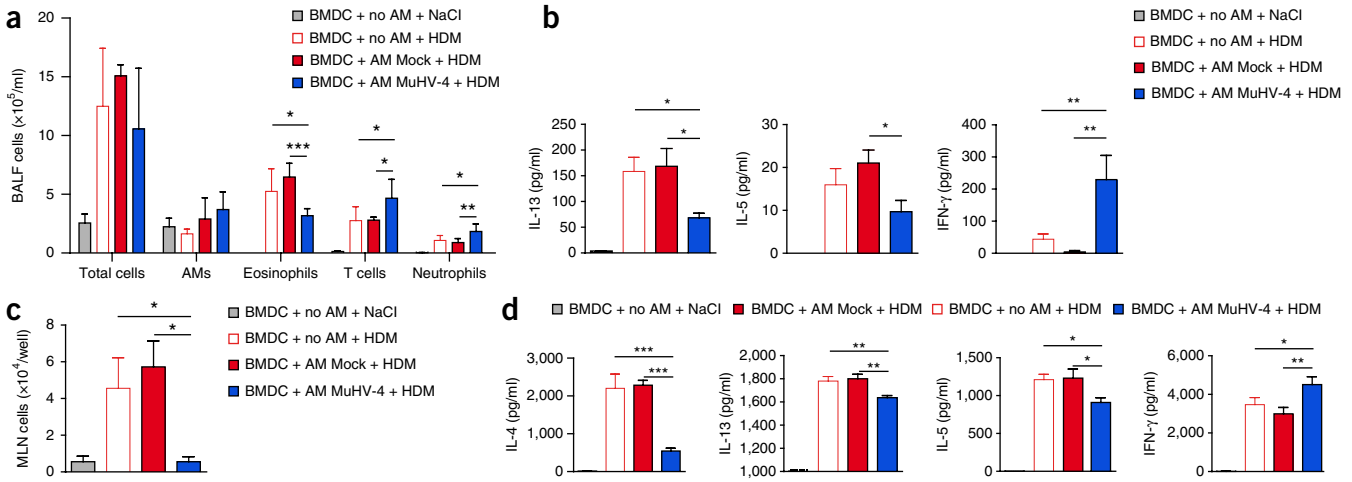

Figure 8 'MuHV-4-imprinted' AMs inhibit the induction of airway allergy by HDM-pulsed BMDCs. (**a**) Total and differential cell counts in BALF from mock-infected recipient BALB/c mice given intranasal transfer of BMDCs cultured for 18 h alone (+ no AM) or with purified AMs (+ AM) from the BALF of donor mice mock infected or infected (for 30 d) with MuHV-4 intranasally, in the presence (HDM) or absence (NaCl) of HDM, and challenged on days 10 and 11 after cell transfer with 10 μg HDM, assessed at euthanasia. (**b**,**c**) ELISA of cytokines in BALF (**b**) and proliferation of MLN cells (**c**) from mice as in **a**. (**d**) ELISA of cytokines in supernatants of MLN cells obtained from mice as in **a** and restimulated for 3 d *ex vivo* with HDM. $^{*}P < 0.05$, $^{**}P < 0.01$ and $^{***}P < 0.001$ (one-way ANOVA and Tukey's multiple-comparison test). Data are representative of three independent experiments with five mice per group (mean + s.e.m.).

reached 55% (corresponding to 90% donor origin) among AMs in MuHV-4-infected mice at day 28 after infection (**Fig. 6b**,**c**), which suggested persistence of the monocyte-derived AMs recruited during infection or continued recruitment from the BM. In a complementary approach, we transferred total BM cells intraperitoneally into newborn pups 11 d of age[39]. Because the lung AM niche is seeded in the first week of life by fetal monocytes[40], this approach generates chimeric mice in which the blood monocytes are derived partially from the donor, while the AMs are of host origin[39]. Chimeric mice were infected intranasally with MuHV-4 at 7 weeks after transfer, and donor chimerism of blood monocytes and AMs was analyzed at days 0 and 28 after infection. Donor chimerism was low (0.3–1.5%) for blood leukocytes and was nearly null (<0.05%) for AMs of mock-infected mice (**Fig. 6d**), while ~80% of AMs were of donor origin in MuHV-4-infected mice at 28 d after infection (**Fig. 6e**,**f**).

To investigate how long the BM-derived macrophages persisted in the lungs after infection with MuHV-4, we sorted BM monocytes from MuHV-4-infected mice at day 5 after infection (corresponding to the peak proportion of $MHCII^{hi}Sca\text{-}1^{+}$ cells; **Fig. 5b**) and transferred them directly into the lungs of MuHV-4-infected mice at day 8 after infection (corresponding to the peak recruitment of monocytes into the lungs and the peak disappearance of resident AMs; **Fig. 5a**) and monitored the maintenance of donor cells into the lungs at days 2, 8, 15 and 28 after transfer. Donor cells in BALF displayed autofluorescence and expression of the integrin CD11c (typical of AMs) from day 2 after transfer, and this was detected up to 28 d after transfer (**Fig. 6g**,**h**). These data indicate that infection with MuHV-4 triggered the recruitment of BM-derived monocytes that replaced the resident AMs and were present in the niche for weeks.

AMs from MuHV-4-infected mice inhibit HDM-induced allergy

To assess the role of AMs in the MuHV-4-induced protection against allergy, we depleted mock- and MuHV-4-infected mice of AMs by intranasal administration of endotoxin-free PBS (as a control) or liposomes containing clodronate (at days 30 and 32 after infection) and subjected the mice to the HDM high-dose model 2 weeks after the final treatment with PBS or clodronate. Both mock HDM mice treated with PBS and mock HDM mice treated with clodronate showed strong and similar airway allergy induction (**Fig. 7a**), which indicated that clodronate treatment did not affect the allergic response in mock HDM mice. In contrast, depleting MuHV-4 HDM mice of AMs with clodronate induced more recruitment of eosinophils into the BALF than that of MuHV-4 HDM mice that did not undergo such depletion (**Fig. 7a**), which indicated that AMs were necessary for the dampening of HDM-induced allergy following infection with MuHV-4. Next, we adoptively transferred AMs from mock- or MuHV-4-infected mice into naive recipient mice. While transfer of AMs from mock-infected mice did not affect subsequent HDM-induced airway allergy, transfer of AMs from MuHV-4-infected mice induced protection, as determined by the reduced number of eosinophils in BALF (**Fig. 7b**). AMs isolated from MuHV-4-infected donor mice showed higher expression of MHC class II than that of AMs from recipient mice (**Fig. 7c**).

Finally, we investigated how MuHV-4-induced BM-derived AMs affected the ability of DCs to trigger HDM sensitization. We isolated AMs from the BALF of mock- or MuHV-4-infected mice at 1 month after infection, cultured those cells together with bone-marrow-derived DCs (BMDCs) and pulsed the cultures for 18 h with HDM. We transferred non-adherent cells into naive 8-week-old female BALB/c mice and challenged those recipient mice with 10 μg HDM at days 10 and 11 after cell transfer. Mice given transfer of HDM-pulsed BMDCs cultured with AMs from MuHV-4-infected mice showed attenuated eosinophilia (**Fig. 8a**) and reduced IL-5 and IL-13 and increased IFN-γ in BALF (**Fig. 8b**) relative to that of recipients of HDM-pulsed BMDCs alone or HDM-pulsed BMDCs cultured with AMs from mock-infected mice. Finally, after restimulation *ex vivo*, MLN cells from mice given transfer of BMDCs cultured with AMs from MuHV-4-infected mice had lower proliferation and lower production of T_H2 cytokines than that of MLN cells isolated from mice given transfer of BMDCs cultured with AMs from mock-infected mice (**Fig. 8c**,**d**). These results indicated that AMs from MuHV-4-infected mice were necessary and sufficient for the dampening of the allergic

response to HDM and were able to block allergic sensitization by BMDCs.

DISCUSSION

Here we showed that respiratory infection with MuHV-4 conferred strong and lasting protection against HDM-induced airway allergy. Respiratory infection with MuHV-4 induced the death of lung-resident AMs and subsequent repopulation of the emptied alveolar niche by BM-derived monocytes that rapidly differentiated into AMs. At 1 month after infection, the vast majority of AMs were BM derived, and these AMs were able to block the ability of DCs to trigger an HDM-specific T_H2 response.

In uninfected mice, resident AMs develop from fetal liver monocytes[40] and are able to self-maintain even after depletion such as that observed after infection with influenza virus[41]. However, in neonatal *Csf2rb*$^{-/-}$ mice, which are deficient in the β-chain of the receptor for the cytokine GM-CSF and lack AMs because of the absence of GM-CSF signaling[42], BM-derived monocytes can colonize the empty alveolar niche and differentiate into AMs that are almost identical transcriptionally to lung-resident AMs derived from fetal-liver monocytes, self-maintain and are fully functional[34]. That observation has prompted the proposal that embryonic and BM precursors of macrophages would have an almost identical potential to develop into resident AMs, if the alveolar niche were available and accessible[37]. Our results showing that BM monocytes colonized the AM niche after infection with MuHV-4 and were maintained for at least 28 d would support such a possibility. Contrary to what was observed at steady state[34], AMs from MuHV-4-infected mice displayed functional properties distinct from those of embryo-derived lung-resident AMs, as they were sufficient to inhibit HDM-induced sensitization. The reason for this functional distinction might reflect differences between embryonic origin and BM origin or might be a consequence of the inflammatory environment caused by infection with MuHV-4 or both.

Recruitment of regulatory monocytes following various types of microbial stimulation has been reported[36,43]. Following acute intestinal infection with *Toxoplasma gondii*, Ly6C^{hi} monocytes recruited into the lamina propria of the small intestine have a regulatory phenotype that is primed in the BM through sensing of IFN-γ[36,44]. We observed that after infection with MuHV-4, a large proportion of blood monocytes expressed IL-10 before reaching the lungs. Moreover, after infection with MuHV-4, monocytes from the BM, blood and BALF displayed increased expression of Sca-1 and MHC class II, which are described as markers of regulatory monocytes following acute intestinal infection with *Toxoplasma gondii*[36]. Future studies should investigate whether infection with MuHV-4 also primes monocyte progenitor cells in the BM for regulatory functions and the mechanism used for this.

Many viruses, in particular persistent viruses such as herpesviruses, induce the expression of regulatory molecules. This is often seen as a way of enhancing infection by suppressing immunological function but could also be beneficial to the host by reducing disease severity. Accordingly, the induction of IL-10 by infection with MuHV-4 increases the viral burden and promotes latency establishment, while at the same time, it limits virus-induced splenomegaly and leukocytosis[45,46]. Here we showed that regulatory monocytes induced by infection with MuHV-4 blocked the development of allergic asthma. The importance of these monocytes in the viral lifecycle will have to be addressed in future studies.

Allergic sensitization is initiated by CD11b$^+$ cDC2s[22,26]. Our functional analysis did not show an effect of infection with MuHV-4 on the ability of these cells to take up HDM, migrate or deliver the allergen in MLNs. However, while T_H2 sensitization against HDM was not observed in MuHV-4 HDM mice, an immune response to HDM developed and displayed T_H1 polarization, as revealed by the inverted balance between IgG-IgE and IgG2c HDM-specific antibodies, the presence of IFN-γ in BALF and IFN-γ production by restimulated MLN cells from MuHV-4 HDM mice. Those observations could be linked to the reduced expression of various maturation markers on CD11b$^+$ cDC2s, such as CD40, CD80 and CD86, as costimulation of DCs with CD80 and CD86 has been shown to be essential during priming of the differentiation of naive T cells into T_H2 cells[47]. How BM-derived AMs affect DCs in MuHV-4-infected mice will have to be delineated in the future.

Together our results have illustrated that the history of infection can have a profound effect on the subsequent development of disease. While much evidence indicates a relationship between severe lower respiratory viral infections early in life and a diagnosis of asthma in later childhood[48], we found that infection with some viruses might profoundly remodel the lung immune system toward a more regulatory environment. In the case of infection with MuHV-4, this remodeling involved the replacement of resident embryonic AMs by recruited Ly6C^{hi} monocytes with a regulatory profile. As AMs are targeted by many infections and are long-lived, these results might provide a mechanistic explanation for the observation that infections during early childhood can orientate the immune response to heterologous antigens such as allergens in the long term. Such understanding might be useful for the development of treatments for protective lung immune responses.

METHODS

Methods, including statements of data availability and any associated accession codes and references, are available in the online version of the paper.

Note: Any Supplementary Information and Source Data files are available in the online version of the paper.

ACKNOWLEDGMENTS

We thank U. Eriksson (Center for Molecular Cardiology, University of Zurich) for BALB/c CD45.1$^+$ genitor mice; A. Osterhaus, T. Marichal and C. Desmet for critical discussions; and L. Dams, C. Delforge, E. Deglaire, C. Espert, A. Guillaume, M. Sarlet and A. Vanderlinden for technical and secretary assistance. Supported by the University of Liège (VIR-IMPRINT ARC), "Fonds de la Recherche Scientifique - Fonds National Belge de la Recherche Scientifique" ("credit de recherche" J007515F; "projet de recherche" T.0195.16; research associate support for B.D.) and Institut MERIEUX (starting grant).

AUTHOR CONTRIBUTIONS

B.M., M.D. and L.G. designed the experiments with the help of H.H., M.G., B.N.L. and F.B.; B.M. and M.D. did most of the experiments and compiled the data; B.M. , M.D., X.X. and L.G. prepared the figures; X.X. performed the transcriptomic and statistical analyses; J.J., C.M., C.S., F.L., and P.M. were involved in specific experiments; B.M., M.D., D.D., H.H., M.G., B.D., A.V., B.N.L., F.B. and L.G. analyzed the data; and B.M., M.D. and L.G. wrote the manuscript.

COMPETING FINANCIAL INTERESTS

The authors declare no competing financial interests.

1. Brodin, P. *et al.* Variation in the human immune system is largely driven by non-heritable influences. *Cell* **160**, 37–47 (2015).
2. Carr, E.J. *et al.* The cellular composition of the human immune system is shaped by age and cohabitation. *Nat. Immunol.* **17**, 461–468 (2016).
3. Netea, M.G. *et al.* Trained immunity: A program of innate immune memory in health and disease. *Science* **352**, aaf1098 (2016).
4. Lambrecht, B.N. & Hammad, H. The immunology of the allergy epidemic and the hygiene hypothesis. *Nat. Immunol.* **18**, 1076–1083 (2017).

5. Lambrecht, B.N. & Hammad, H. The immunology of asthma. *Nat. Immunol.* **16**, 45–56 (2015).
6. Beura, L.K. *et al.* Normalizing the environment recapitulates adult human immune traits in laboratory mice. *Nature* **532**, 512–516 (2016).
7. Webley, W.C. & Aldridge, K.L. Infectious asthma triggers: time to revise the hygiene hypothesis? *Trends Microbiol.* **23**, 389–391 (2015).
8. Nilsson, C. *et al.* Does early EBV infection protect against IgE sensitization? *J. Allergy Clin. Immunol.* **116**, 438–444 (2005).
9. Saghafian-Hedengren, S., Sverremark-Ekström, E., Linde, A., Lilja, G. & Nilsson, C. Early-life EBV infection protects against persistent IgE sensitization. *J. Allergy Clin. Immunol.* **125**, 433–438 (2010).
10. Balfour, H.H. Jr. *et al.* Age-specific prevalence of Epstein-Barr virus infection among individuals aged 6-19 years in the United States and factors affecting its acquisition. *J. Infect. Dis.* **208**, 1286–1293 (2013).
11. Condon, L.M. *et al.* Age-specific prevalence of Epstein-Barr virus infection among Minnesota children: effects of race/ethnicity and family environment. *Clin. Infect. Dis.* **59**, 501–508 (2014).
12. Dowd, J.B., Palermo, T., Brite, J., McDade, T.W. & Aiello, A. Seroprevalence of Epstein-Barr virus infection in U.S. children ages 6-19, 2003-2010. *PLoS One* **8**, e64921 (2013).
13. Cesarman, E. Gammaherpesviruses and lymphoproliferative disorders. *Annu. Rev. Pathol.* **9**, 349–372 (2014).
14. Virgin, H.W., Wherry, E.J. & Ahmed, R. Redefining chronic viral infection. *Cell* **138**, 30–50 (2009).
15. Barton, E.S. *et al.* Herpesvirus latency confers symbiotic protection from bacterial infection. *Nature* **447**, 326–329 (2007).
16. Reese, T.A. *et al.* Sequential infection with common pathogens promotes human-like immune gene expression and altered vaccine response. *Cell Host Microbe* **19**, 713–719 (2016).
17. MacDuff, D.A. *et al.* Phenotypic complementation of genetic immunodeficiency by chronic herpesvirus infection. *eLife* **4**, 4 (2015).
18. Barton, E., Mandal, P. & Speck, S.H. Pathogenesis and host control of gammaherpesviruses: lessons from the mouse. *Annu. Rev. Immunol.* **29**, 351–397 (2011).
19. Hammad, H. *et al.* House dust mite allergen induces asthma via Toll-like receptor 4 triggering of airway structural cells. *Nat. Med.* **15**, 410–416 (2009).
20. Cadwell, K. The virome in host health and disease. *Immunity* **42**, 805–813 (2015).
21. Fowler, P., Marques, S., Simas, J.P. & Efstathiou, S. ORF73 of murine herpesvirus-68 is critical for the establishment and maintenance of latency. *J. Gen. Virol.* **84**, 3405–3416 (2003).
22. Plantinga, M. *et al.* Conventional and monocyte-derived CD11b^{+} dendritic cells initiate and maintain T helper 2 cell-mediated immunity to house dust mite allergen. *Immunity* **38**, 322–335 (2013).
23. Hammad, H. *et al.* Inflammatory dendritic cells--not basophils--are necessary and sufficient for induction of Th2 immunity to inhaled house dust mite allergen. *J. Exp. Med.* **207**, 2097–2111 (2010).
24. van Helden, M.J. & Lambrecht, B.N. Dendritic cells in asthma. *Curr. Opin. Immunol.* **25**, 745–754 (2013).
25. Guilliams, M. *et al.* Dendritic cells, monocytes and macrophages: a unified nomenclature based on ontogeny. *Nat. Rev. Immunol.* **14**, 571–578 (2014).
26. Mesnil, C. *et al.* Resident CD11b^{+}Ly6C^{-} lung dendritic cells are responsible for allergic airway sensitization to house dust mite in mice. *PLoS One* **7**, e53242 (2012).
27. Holt, P.G., Haining, S., Nelson, D.J. & Sedgwick, J.D. Origin and steady-state turnover of class II MHC-bearing dendritic cells in the epithelium of the conducting airways. *J. Immunol.* **153**, 256–261 (1994).
28. Hussell, T. & Bell, T.J. Alveolar macrophages: plasticity in a tissue-specific context. *Nat. Rev. Immunol.* **14**, 81–93 (2014).
29. Bedoret, D. *et al.* Lung interstitial macrophages alter dendritic cell functions to prevent airway allergy in mice. *J. Clin. Invest.* **119**, 3723–3738 (2009).
30. Holt, P.G. *et al.* Downregulation of the antigen presenting cell function(s) of pulmonary dendritic cells in vivo by resident alveolar macrophages. *J. Exp. Med.* **177**, 397–407 (1993).
31. Lauzon-Joset, J.F., Marsolais, D., Langlois, A. & Bissonnette, E.Y. Dysregulation of alveolar macrophages unleashes dendritic cell-mediated mechanisms of allergic airway inflammation. *Mucosal Immunol.* **7**, 155–164 (2014).
32. Lawler, C., Milho, R., May, J.S. & Stevenson, P.G. Rhadinovirus host entry by co-operative infection. *PLoS Pathog.* **11**, e1004761 (2015).
33. Spinelli, L., Carpentier, S., Montañana Sanchis, F., Dalod, M. & Vu Manh, T.P. BubbleGUM: automatic extraction of phenotype molecular signatures and comprehensive visualization of multiple Gene Set Enrichment Analyses. *BMC Genomics* **16**, 814 (2015).
34. van de Laar, L. *et al.* Yolk sac macrophages, fetal liver, and adult monocytes can colonize an empty niche and develop into functional tissue-resident macrophages. *Immunity* **44**, 755–768 (2016).
35. Gibbings, S.L. *et al.* Transcriptome analysis highlights the conserved difference between embryonic and postnatal-derived alveolar macrophages. *Blood* **126**, 1357–1366 (2015).
36. Askenase, M.H. *et al.* Bone-marrow-resident NK cells prime monocytes for regulatory function during infection. *Immunity* **42**, 1130–1142 (2015).
37. Guilliams, M. & Scott, C.L. Does niche competition determine the origin of tissue-resident macrophages? *Nat. Rev. Immunol.* **17**, 451–460 (2017).
38. Shi, C. & Pamer, E.G. Monocyte recruitment during infection and inflammation. *Nat. Rev. Immunol.* **11**, 762–774 (2011).
39. Scott, C.L. *et al.* Bone marrow-derived monocytes give rise to self-renewing and fully differentiated Kupffer cells. *Nat. Commun.* **7**, 10321 (2016).
40. Guilliams, M. *et al.* Alveolar macrophages develop from fetal monocytes that differentiate into long-lived cells in the first week of life via GM-CSF. *J. Exp. Med.* **210**, 1977–1992 (2013).
41. Hashimoto, D. *et al.* Tissue-resident macrophages self-maintain locally throughout adult life with minimal contribution from circulating monocytes. *Immunity* **38**, 792–804 (2013).
42. Schneider, C. *et al.* Induction of the nuclear receptor PPAR-γ by the cytokine GM-CSF is critical for the differentiation of fetal monocytes into alveolar macrophages. *Nat. Immunol.* **15**, 1026–1037 (2014).
43. Sabatel, C. *et al.* Exposure to bacterial CpG DNA protects from airway allergic inflammation by expanding regulatory lung interstitial macrophages. *Immunity* **46**, 457–473 (2017).
44. Grainger, J.R. *et al.* Inflammatory monocytes regulate pathologic responses to commensals during acute gastrointestinal infection. *Nat. Med.* **19**, 713–721 (2013).
45. Peacock, J.W. & Bost, K.L. Murine gammaherpesvirus-68-induced interleukin-10 increases viral burden, but limits virus-induced splenomegaly and leukocytosis. *Immunology* **104**, 109–117 (2001).
46. Siegel, A.M., Herskowitz, J.H. & Speck, S.H. The MHV68 M2 protein drives IL-10 dependent B cell proliferation and differentiation. *PLoS Pathog.* **4**, e1000039 (2008).
47. van Rijt, L.S. *et al.* Essential role of dendritic cell CD80/CD86 costimulation in the induction, but not reactivation, of TH2 effector responses in a mouse model of asthma. *J. Allergy Clin. Immunol.* **114**, 166–173 (2004).
48. Busse, W.W., Lemanske, R.F. Jr. & Gern, J.E. Role of viral respiratory infections in asthma and asthma exacerbations. *Lancet* **376**, 826–834 (2010).

ONLINE METHODS

Reagent. Extracts of lyophilized HDM (*Dermatophagoides farinae*) were from Greer Laboratories.

Cells. BHK-21 fibroblasts (ATCC CCL-10) were cultivated on DMEM supplemented with 2 mM glutamine, 100 U/ml penicillin, 100 mg/ml streptomycin and 10% FCS. For *ex vivo* experiments, cells were maintained in RPMI 1640 medium containing Glutamax-I with 10% FCS, 50 μM 2-mercaptoethanol, 100 U/ml penicillin and 100 mg/ml streptomycin. Cells were free of mycoplasma contamination.

Viruses. The wild-type MHV-68 strain of MuHV-4 (ref. 49) was used, as was latency-deficient MHV68 mutants (MuHV-4 FS73 and MuHV-4 Del73) and the corresponding revertant (MuHV-4 Rev73)[21]. Viral stocks were grown on BHK (baby hamster kidney) cells and were purified and titrated as described[50].

Mice. Female BALB/c or C57BL/6 wild-type mice were purchased from Envigo (Venray, Netherlands). Mice with transgenic expression of the β-chain of the T cell antigen receptor (1-DERβ mice) were described previously[22]. BALB/c CD45.1$^+$ genitor mice were provided by U. Eriksson (Center for Molecular Cardiology, University of Zurich). Except where stated otherwise, all mice used were 8 weeks of age. Animals were housed in the University of Liege according to the guidelines of the European Convention for the Protection of Vertebrate Animals used for Experimental and other Scientific Purposes (CETS 123). The protocol was approved by the Committee on the Ethics of Animal Experiments of the University of Liege (permit number 1276). Before each experiment, mice were randomly assigned to the various groups. No blinding analysis was performed.

Mouse infection. Intranasal or intraperitoneal administration of virions was performed under isoflurane anesthesia, with 1×10^4 PFU in 50 μl of PBS. As control, mock-infected mice received 50 μl of PBS. Pulmonary infectious virus was assessed by plaque assay on lung homogenates. Quantification of antibodies to MuHV-4 by ELISA and quantification of MuHV-4 genomic and cellular DNA copies by quantitative PCR were performed as described[51].

Administration of HDM extracts. Isoflurane anesthetized mice received intranasal instillation of LPS-free saline or HDM in 50 μl. To induce allergic airway inflammation, two different protocols were used. In the high-dose protocol, mice were treated with 100 μg HDM extracts on day 0 and were subsequently challenged with 100 μg HDM on days 7 and 14. In an alternative protocol (HDM low-dose), mice were sensitized with 10 μg HDM on day 0 and were subsequently challenged with 10 μg HDM on days 7 to 11. In both models, analyses were performed on euthanized mice 3 d after the final HDM administration. To assess the early innate response to HDM, mice were sensitized with 100 μg HDM and were euthanized after 1, 2 or 3 d. To assess HDM uptake and DC migration upon HDM sensitization, HDM labeled with an AlexaFluor647 labeling kit (Invitrogen) was used to sensitize the mice.

Lung histology. Lungs were fixed in 5% formalin, paraffin embedded and cut into 5-μm sections that were then stained with either hematoxylin-eosin or periodic acid Schiff before microscopic analysis (Leica Microsystems).

BAL, cytology and cytokine measurement. After euthanasia, the trachea was catheterized and BAL was performed by two consecutive flushes of the lungs with 1 ml of ice-cold PBS containing EDTA and protease inhibitors. Cell density in BALF was evaluated using a hemocytometer after Tuerk solution staining (Sigma-Aldrich). Differential cell counts in BALF were performed on cytospin preparations stained with May-Grünwald-Giemsa (Merck Millipore) or were determined by flow cytometry. Cytokine production was measured by specific ELISA (Ready-SET-Go, eBioscience) or via magnetic beads-based multiplex immunoassays (ProcartaPlex, eBioscience).

ELISA of HDM-specific IgE, IgG1 and IgG2c. Maxisorp ELISA plates (Nalgene Nunc) were coated overnight with 100 μl per well of 10 μg/ml HDM extracts dissolved in carbonate buffer (pH 9.6, 0.1 M). The next day, plates were washed with 0.05% Tween 20 in PBS and were blocked for 1 h with 150 μl per well of 10% FCS in PBS. Blocking solution was then removed, replaced with mouse sera diluted 1/20 in blocking solution and incubated for 2 h at room temperature. Wells were washed and then incubated for 1 h with 100 μl per well of 10 μg/ml biotinylated rat anti-mouse IgE (BD Pharmingen, Clone R35-118), biotinylated goat anti-mouse IgG1 (Southern Biotech, Cat. No. 1070-08) or biotinylated goat anti-mouse IgG2c (Southern Biotech, Cat. No. 1079-08), all diluted in blocking solution. That was followed by incubation with streptavidin-conjugated horseradish peroxidase (Dako) for 1 h. After a final wash step, 100 μl TMB substrate (eBioscience) was added, and the reaction was stopped with 50 μl 0.5M H_2SO_4. The absorbance was read at 450 nm using an iMarkTM ELISA microplate reader (Bio-Rad).

Cell suspension preparations from organs. To harvest lung cells, mice were perfused with ice-cold PBS through the right ventricle. Then, lung lobes were collected into a C-Tube (Miltenyi) containing complete HBSS medium,1 mg/ml collagenase D (Roche) and 50 μg/ml DNase I (Roche), then were processed with a gentleMACS dissociator (Miltenyi) and, finally, were incubated for 30 min at 37 °C. BM cells were obtained from adult mice by crushing the femurs and tibiae. Blood was acquired by cardiac puncture and was immediately suspended in ice-cold PBS complemented with 5 mM EDTA. Suspensions of cells were finally washed and treated for lysis of the erythrocytes (red lysis buffer, eBioscience). For MLN cells, MLNs were harvested after euthanasia, and single-cell suspensions were prepared using sterile syringe plunger. For all preparations, cells were finally strained through a 70-μm filter.

Flow cytometry. Labeling of single-cell suspension was performed on ice in PBS containing 2% fetal bovine albumin and 2mM EDTA. Cells were first incubated for 20 min with a purified rat IgG2a anti-mouse CD16/CD32 antibody (eBioscience) to block Fc binding. Flow-cytometry staining was performed for 30 min at 4 °C in PBS containing 0.5% BSA with various panels of fluorochrome-conjugated antibodies: antibodies to CD45 (30-F11, BV510 or PE-Cy7), CD45.1 (A20, APC), CD45.2 (104, V500), MHC-II (M5/114.15.2, PerCP-Cy5.5), CD3e (17A2, V450 or 145-2C11, APC-Cy7), CD8 (53-6.7, AlexaFluor488), CD19 (MB19-1, APC-Cy7), Ly6G (1A8, APC-H7), SiglecF (E50-2440, AlexaFluor647 or PE), CD11b (M1/70, BV711), CD103 (M290, BV421), CCR7 (4B12, BV421) and CD64 (X54-5/7.1.1, PE or AlexaFluor647), all from BD Biosciences; antibodies to CD16/32 (clone 93, unconjugated), MHC-II (M5/114.15.2, PE-Cy7 or efluor 450), CD3e (145-2C11, APC), CD4 (RM 4-5, PerCP-Cy5.5 and FITC), CD19 (MB19-1, APC), Gr-1 (RB6-8C5, FITC), CD11c (N418, PerCP-Cy5.5 or AlexaFluor700), CD11b (M1/70, APC-eFluor780), CD103 (2E7, FITC), Ly6C (HK1.4, PE or PE-Cy7), CD86 (GL1, PE), CD40 (1C10, PE), CD80 (16-10A1, PE) and Ly6A/E (D7, FITC), all from eBioscience; antibodies to CD11b (M1/70, BV711) and Ly6C (HK1.4, BV785), both from BioLegend; and antibody to CCR2 (475301, PE), from R&D Systems. For some experiments, Alexa Fluor 647–conjugated HDM (HDM-647) was included in the panel design. For experiments assessing expression of DC maturation markers, single staining for surface antigens was performed by mixture of MLN cells from mock- and MuHV-4-infected mice. Indeed, as population expansion of B cells following infection with MuHV-4 (ref. 18) could have decreased the availability of antibodies to these surface antigens, MLN cells from MuHV-4-infected mice were labeled with CFSE (0.05 μM, CellTrace CFSE Cell Proliferation Kit, ThermoFisher, C34554) and were mixed with mock CFSE$^-$ MLN cells before cell surface staining and flow cytometry, to avoid any artefactual interpretation in MFI comparisons (**Supplementary Fig. 5**). As a control, the reciprocal experiment was performed (data not shown). Samples were processed on a BD LSR Fortessa X-20 or were sorted by a FACSAria IIIu (BD Biosciences) (both equipped with 50-mW violet 405-nm, 50-mW blue 488-nm, 50-mW yellow-green 561-nm and 40-mW red 633-nm lasers and an ND1.0 filter in front of the FSC photodiode).

IL-10 secretion assay. To identify IL-10-secreting cells, a cytokine-secretion assay (Miltenyi Biotec) was performed. Blood and BALF leucocytes were isolated, and single-cell suspensions were prepared as described

above. Samples were incubated with HDM (30 μg/ml) for 3 h at 37 °C before being processed according to the manufacturer's instructions and were analyzed by flow cytometry.

MLN cell restimulation, proliferation assay and cytokine production. 2×10^5 MLN cells were restimulated for 72 h in the presence or absence of 30 μg/ml HDM extracts. The proliferation was measured as [^{3}H]thymidine incorporation during the final 16 h of a 3-day culture or was quantified as the increased number of cells compared to the unstimulated corresponding controls (described as MLN cell population expansion). Cytokine concentrations were measured using the Ready-Set-Go ELISA sets (eBioscience).

DCs transfer. MLNs from mock- or MuHV-4-infected BALB/c mice were harvested 3 d after sensitization with a high dose of HDM (100 μg), and single-cell suspensions were prepared using standard methods. MLN CD11c$^+$ cells were purified with CD11c microbeads (Miltenyi Biotech) according to the manufacturer's protocol and were injected (1×10^5) intranasally in 75 μl of PBS into naive recipient BALB/c mice under isoflurane anesthesia. Recipient mice were challenged with 10 μg HDM 9 d after transfer and were euthanized 3 d after challenge to assess development of airway inflammation.

Transfer of HDM-specific CD4$^+$ T cells. CD4$^+$ T cells were isolated from the spleen of 1-DERβ mice and were stained with 5 μM of CFSE according to the manufacturer's protocol (CellTrace CFSE Cell Proliferation Kit, Thermo Fisher). The CFSE-stained CD4$^+$ T cells were injected intravenously into C57BL/6 recipient mice, under isoflurane anesthesia, that had been mock infected or infected for 30 d with MuHV-4. Recipient mice were concomitantly sensitized with 10 μg HDM and were euthanized 3 d later to evaluate the proliferation of 1-DERβ CD4$^+$ T cells.

AM isolation and transfer. AMs were purified by positive CD11c MACS selection (Miltenyi Biotech), according to the manufacturer's protocol, from BALF of mock- or MuHV-4-infected mice 30 d after infection. AM purity was checked by flow cytometry (autofluorescent CD11c$^+$ living cells) and was confirmed to be >95%. For transfer experiments, 8×10^5 AMs in 75 μl of PBS were injected intranasally into naive CD45.1$^+$ congenic BALB/c mice under isoflurane anesthesia. 3 d after AM transfer, recipient mice were treated with the HDM high-dose model (100 μg) as described above.

Generation of BMDCs, AM-BMDC coculture and adoptive transfer. BM cells from naive BALB/c mice were grown in RPMI 1640 medium containing Glutamax-I with 10% FCS, 50 μM 2-mercaptoethanol, 100 U/ml penicillin, 100 mg/ml streptomycin and 10 ng/ml recombinant murine GM-CSF (PromoKine). BM cells were plated onto tissue culture plastic and then were cultured, with exchange of half of the medium every other day. After 7 d, control of DC differentiation was performed, before the addition of AMs and HDM pulsing. Isolated AMs from naive BALB/c mice were added to BMDCs at a 1:1 ratio, and *ex vivo* coculture was performed for 18 h. HDM extracts (30 μg/ml) were added to culture medium (without GM-CSF) for the final 12 h to pulse BMDCs. After overnight incubation, non-adherent cells were harvested, washed twice with PBS and injected intranasally (4×10^5 cells in 75 μl of PBS) into naive recipient mice under isoflurane anesthesia. Recipient mice were challenged with two instillations of 10 μg HDM 9 and 10 d after the adoptive transfer and were euthanized 3 d after challenge to assess the development of airway inflammation.

Generation of BM chimeras. BM chimeras were constructed by exposure of BALB/c CD45.2$^+$ mice to a lethal irradiation protocol that preserves the thoracic cavity. These recipient mice were then given intravenous injection of 5×10^6 BM cells isolated from the femur and tibia of BALB/cCD45.1$^+$CD45.2$^+$ congenic donors. The host mice were given broad-spectrum antibiotics (endotrim; Ecuphar), at a concentration of 1.5 mg/ml, for 4 weeks in drinking water. Chimeric mice were allowed to 'rest' for 8 weeks before further experimental manipulation.

Mouse irradiation protocol. A dose of 7 Gy in one fraction was delivered to the whole body, sparing the thoracic cavity, with a dedicated small animal radiotherapy device (SmART Irradiator from Precision X-Ray Inc). Radiation was delivered using a photon beam (maximum energy of 225 kV and 13 mA), which provided a dose rate of 3 Gy/min. The planning system SmART-plan (version 1.3.9 Precision X-ray, North Branford, CT) was used to establish and deliver the treatment. To target the whole body except the thoracic cavity, we used two opposite beams to irradiate the head, and the same schedule to irradiate the abdominal cavity. The dose delivered was almost 0 Gy to the lungs, 7.5 Gy to the soft tissue and 20.5 Gy to the bones. Fluoroscopy was used to check mouse positioning before each beam to avoid thoracic irradiation. During irradiation, mice received continuous isoflurane anesthesia gas via a nose cone (0.4 l/min oxygen with 1.5% isoflurane).

Adoptive transfer to neonates. A total of 8×10^6 CD45.1$^+$ BM cells in 50 μl PBS were injected intraperitoneally once tino 11-day-old CD45.2$^+$ wild-type pups. Mice were killed 8–12 weeks later, and the CD45.1$^+$ donor-derived cells were identified.

AM depletion. 75 μl of a 30% solution of clodronate-containing liposomes in endotoxin-free PBS was administered intranasally to isoflurane-anesthetized mice twice at 2-day intervals. Instillation of 75 μl of endotoxin-free PBS was used as a control. AMs depletion was monitored by flow cytometry 2 d after the final clodronate-liposome instillation.

BM monocytes transfer. For BM monocyte transfer, cells were isolated from CD45.2$^+$ donor femora and tibiae as described above. Samples were depleted of Ly6G$^+$ and CD19$^+$ cells using MACS beads (Miltenyi Biotec), according to the manufacturer's protocol. BM monocytes (live, CD19$^-$Ly6G$^-$CD3$^-$SigleF$^-$CD11b$^+$Ly6C^{hi}CCR2$^+$ cells) were then purified by high-speed sorting using a FACSAria (BD Biosciences). 2×10^5 BM monocytes (in 75 μl of PBS) were transferred intranasally into CD45.1$^+$ congenic BALB/c mice, which infected intranasally with MuHV-4 for 8 d. Maintenance of CD45.2$^+$ donor cells in the lungs was monitored by flow cytometry of BALF cells isolated at days 2, 8, 15 and 28 after transfer.

Transcriptomics analysis of AMs. AMs were isolated as described above from mock- or MuHV-4-infected BALB/c mice at 24 h after a single instillation of 100 μg HDM. RNA from AMs was extracted using the RNeasy Mini kit (Qiagen) according to the manufacturer's instructions, and quality was assessed on a 2100 Agilent Bioanalyzer. RNA-Seq libraries were prepared from 2 μg of RNA, each obtained by pooling 1 μg from two mice (which therefore led to three independent replicates per group), using the Illumina paired-end RNA-Seq library preparation kit. Libraries were finally sequenced and bioinformatics analysis was performed. Approximately 30×10^6 75-base single-end reads were generated per sample. Quality-control checks on raw sequencing data for each sample were performed using FastQC (http://www.bioinformatics.babraham.ac.uk/projects/fastqc/). Reads were mapped to the mouse reference genome (mm10) using STAR (version 2.4.0)[52]. Subsequently, the analysis was performed with R Bioconductor packages[53]. Rsamtools (version 1.18.3) and GenomicAlignments (version 1.2.2) were used to count the reads by exons, and data set counts were then analyzed with edgeR (version 3.8.6) to determine genes expressed differentially. A gene was considered to be expressed differentially with a false-discovery rate of 1×10^{-5} and twofold change $\geq \pm 1$ ($\log_2$ values). RNA-Seq libraries yielded roughly 30×10^6 75-base single reads. In total, more than 85% of reads mapped uniquely to the genome within exons of known genes (**Supplementary Fig. 7a**). We validated sample purity by assessing the expression of lineage-restricted marker genes for potential contaminants, eosinophils, neutrophils, B cells and T cells (**Supplementary Fig. 7b**), which confirmed negligible contamination by non-myeloid cells. Hierarchical clustering of global gene-expression profiles grouped RNA-Seq libraries according to biological condition confirmed the quality and reproducibility of our analysis (**Supplementary Fig. 7c**). Using a *P* value of 1×10^{-5} and a change in expression of at least twofold, we identified 1,368 genes that were expressed differentially (**Supplementary Fig. 7d**). Bubblegum analysis was used as described previously[33] with default settings and the gene sets described in **Supplementary Tables 1** and **2**, as well as with the gene sets GSE5099_CLASSICAL_M1_VS_ALTERNATIVE_M2_MACROPHAGE_UP, GSE5099_CLASSICAL_M1_VS_ALTERNATIVE_M2_MACROPHAGE_DN and KEGG mmu04612. Some of these gene sets were arbitrarily determined

doi:10.1038/ni.3857

based on literature. For these data, Benjamini-Hochberg adjusted *P* values were calculated using the R package DESeq2.

Statistical analysis. $n \geq 5$ mice in each experimental group. Pilot studies were used for estimation of the sample size to ensure adequate power. There was no exclusion of data points or mice. No randomization or blinding was used.

A **Life Science Reporting Summary** for this paper is available.

Data availability. The data that support the findings of this study are available from the corresponding author upon request.

49. Blaskovic, D., Stanceková, M., Svobodová, J. & Mistríková, J. Isolation of five strains of herpesviruses from two species of free living small rodents. *Acta Virol.* **24**, 468 (1980).
50. Machiels, B., Stevenson, P.G., Vanderplasschen, A. & Gillet, L. A gammaherpesvirus uses alternative splicing to regulate its tropism and its sensitivity to neutralization. *PLoS Pathog.* **9**, e1003753 (2013).
51. Latif, M.B. *et al.* Deletion of murid herpesvirus 4 ORF63 affects the trafficking of incoming capsids toward the nucleus. *J. Virol.* **90**, 2455–2472 (2015).
52. Dobin, A. *et al.* STAR: ultrafast universal RNA-seq aligner. *Bioinformatics* **29**, 15–21 (2013).
53. Gentleman, R.C. *et al.* Bioconductor: open software development for computational biology and bioinformatics. *Genome Biol.* **5**, R80 (2004).

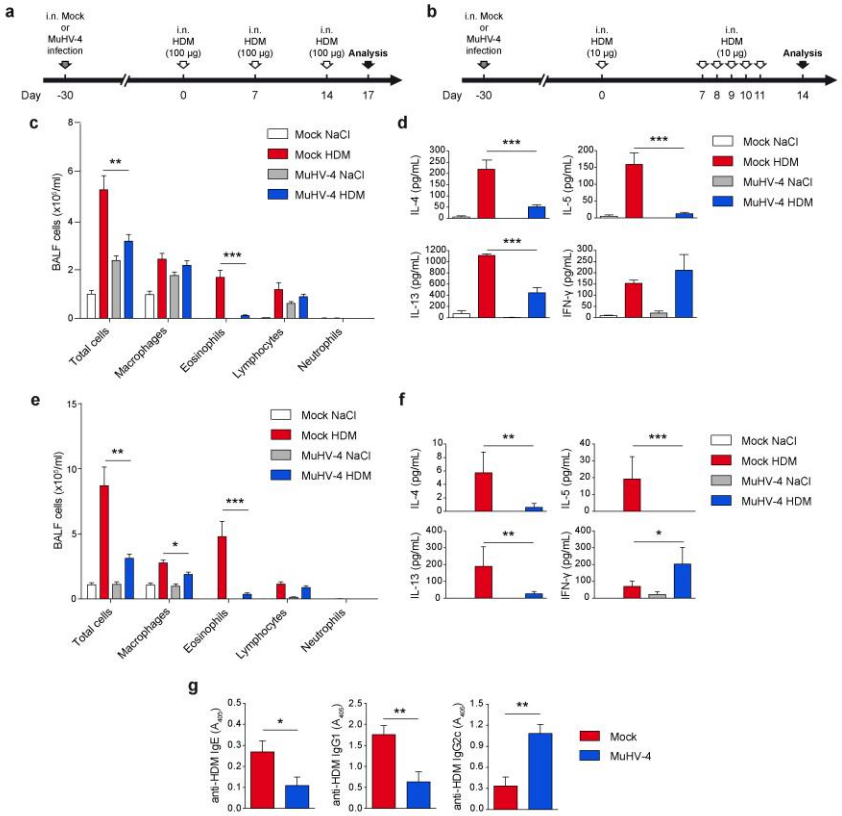

Supplementary Figure 1

Infection with MuHV-4 protects both BALB/c and C57BL/6 mice against HDM-induced allergic asthma.

(**a**) Experimental design of HDM-induced high dose model of asthma in BALB/c mice. Mice were mock-infected or infected intranasally with MuHV-4 ($1x10^4$ PFU in 50 µL PBS). Thirty days post-infection (p.i.), animals received 3 sequential intranasal instillations of saline or 100 µg HDM extracts (day 0, 7, 14) before euthanasia and airway allergy evaluation 3 days later (day 17). (**b**) Experimental design of HDM-induced low dose model of asthma in BALB/c or C57BL/6. Thirty days p.i. as in **a**, animals received intranasal saline instillation or were sensitized with 10 µg HDM (day 0). One week later, mice were challenged with 5 daily intranasal instillations of 10 µg HDM (days 7 to 11) before euthanasia and airway allergy evaluation 3 days after the last instillation (day 14). (**c-g**) Total and differential cell counts of BALF cells (**c,e**), ELISA measurement of cytokine release by MLN cells following *ex vivo* restimulation with HDM (**d,f**), and ELISA Measurement of HDM-specific IgE, IgG1 and IgG2c levels in sera (**g**) at euthanasia of mock or MuHV-4-infected BALB/c (**c-d**) or C57BL/6 mice (**e-g**), submitted 30 days p.i. to the HDM-induced low dose model of asthma (as in **b**). *** p< 0.001, ** p< 0.01 and * p < 0.05 (Two-way ANOVA and Tukey's multiple comparison test (c-e) or Student's t-test (g)). Data are representative of 2 independent experiments with 5 mice per group (mean ± s.e.m. in **c-g**).

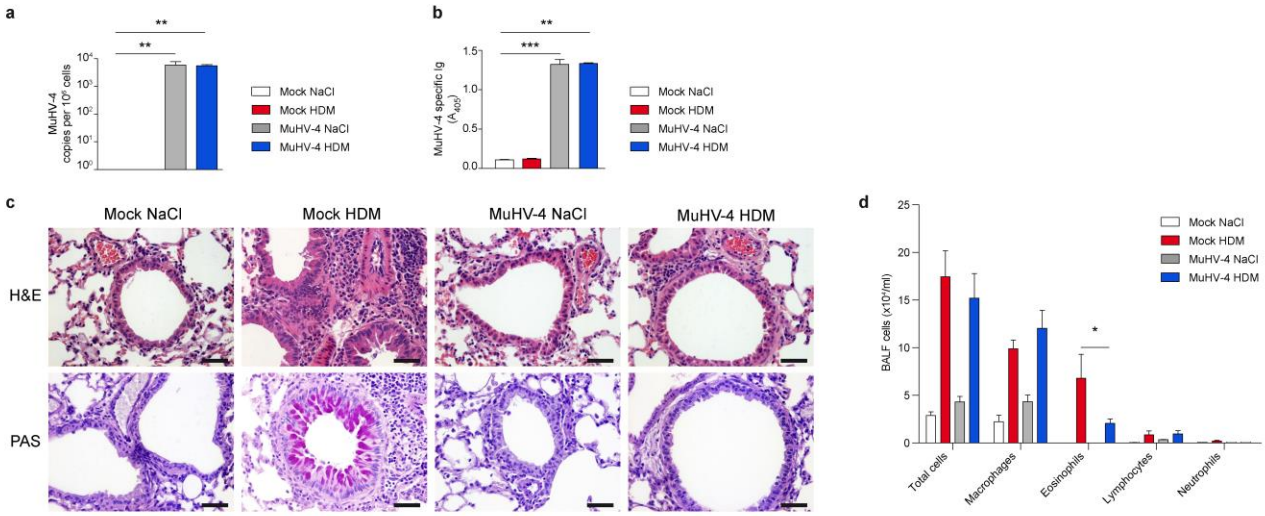

Supplementary Figure 2

Infection with MuHV-4 impairs HDM-induced airway allergy in young mice.

(**a-d**) Quantification of MuHV-4 genomic copies in splenic cells by qPCR (**a**) and of MuHV-4 specific immunoglobulins in sera by ELISA (**b**), histological analysis of lung sections (scale bars, 100 µm) (**c**), total and differential cell counts of BALF cells (**d**), at euthanasia of mock or MuHV-4-infected 3 weeks old BALB/c mice, submitted 30 days p.i. to the HDM-induced high dose model of asthma. Data are mean ± s.e.m. of samples from 5 mice per group. *** p< 0.001, ** p< 0.01 and * p < 0.05 (Two-way (**a, b**) or One-way (**d**) ANOVA and Tukey's multiple comparison test).

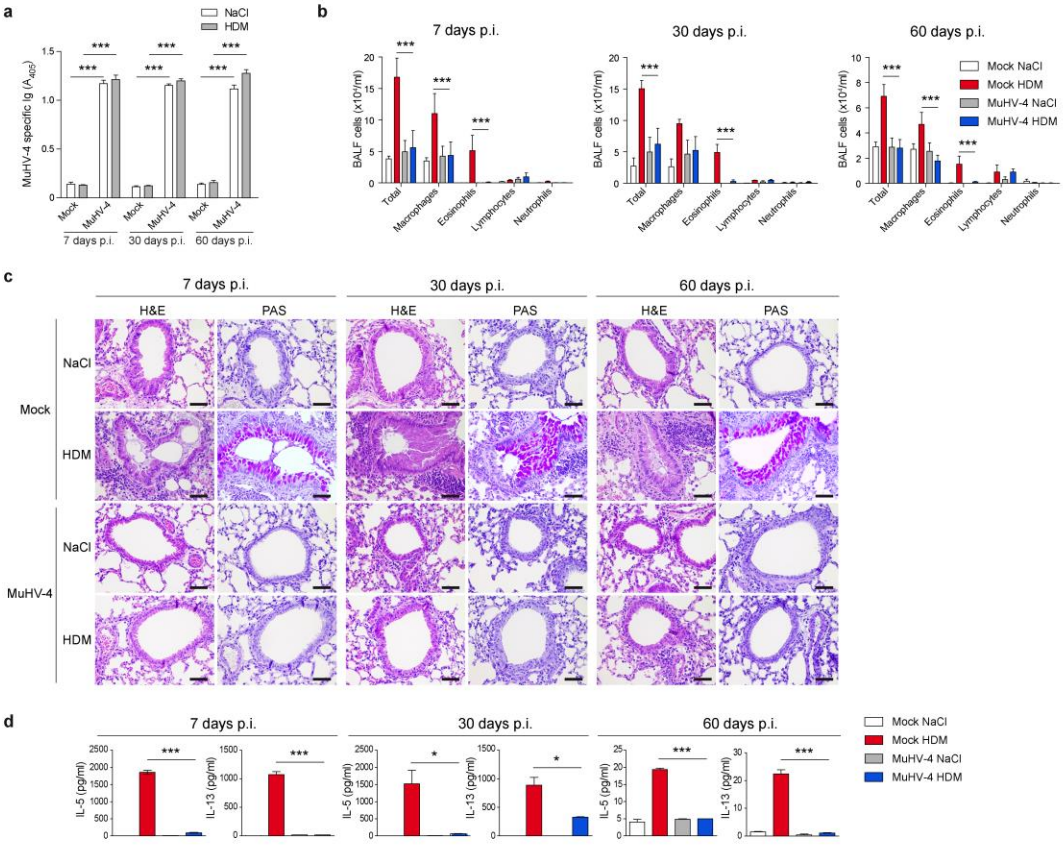

Supplementary Figure 3

Infection with MuHV-4 induces a long-term protection against HDM-induced airway allergy.

(**a-d**) Quantification of MuHV-4 specific immunoglobulins in sera by ELISA (**a**), total and differential cell counts of BALF cells (**b**), histological analysis of lung sections (scale bars, 100 µm) (**c**), and ELISA measurement of cytokine release by MLN cells following *ex vivo* restimulation by HDM (**d**), at euthanasia of mock or MuHV-4-infected BALB/c mice, submitted 7, 30 or 60 days p.i. to the HDM-induced high dose model of asthma. *** p< 0.001, ** p< 0.01 and * p < 0.05 (Two-way ANOVA and Tukey's multiple comparison test). Data are representative of two independent experiments with 5 mice per group (mean ± s.e.m. in **a, b, d**).

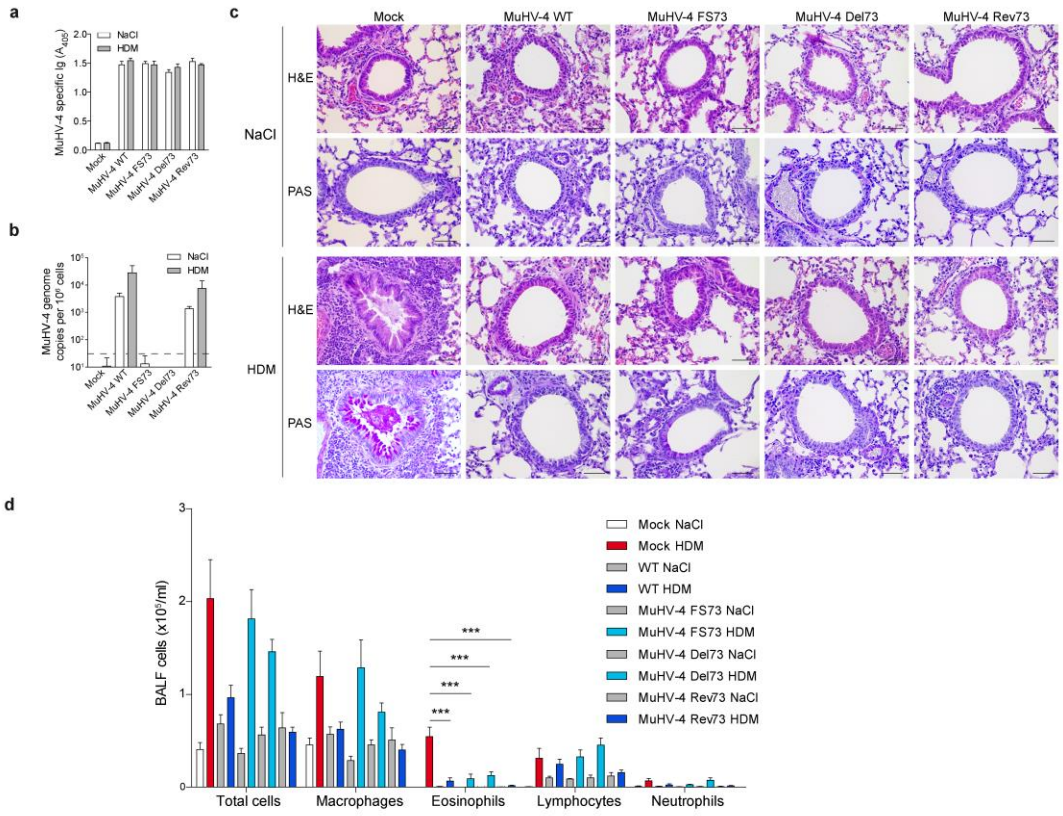

Supplementary Figure 4

Establishment of MuHV-4 latency is not necessary to allow protection against HDM-induced airway allergy.

(**a-d**) Quantification of MuHV-4 specific immunoglobulins in sera by ELISA (**a**), quantification of MuHV-4 genomic copies in splenic cells by qPCR (**b**), histological analysis of lung sections (scale bars, 100 µm) (**c**), and total and differential cell counts of BALF cells (**d**) at euthanasia of mock or MuHV-4-infected BALB/c mice either with the WT strain or with latency-deficient viral mutants (FS73 and Del73 strains) or with a corresponding revertant (Rev73), submitted 30 days p.i. to the HDM-induced high dose model of asthma. *** $p < 0.001$, ** $p < 0.01$ and * $p < 0.05$ (Two-way ANOVA and Tukey's multiple comparison test). Data are representative of 2 independent experiments with 5 mice per group (mean ± s.e.m. in **a,b,d**).

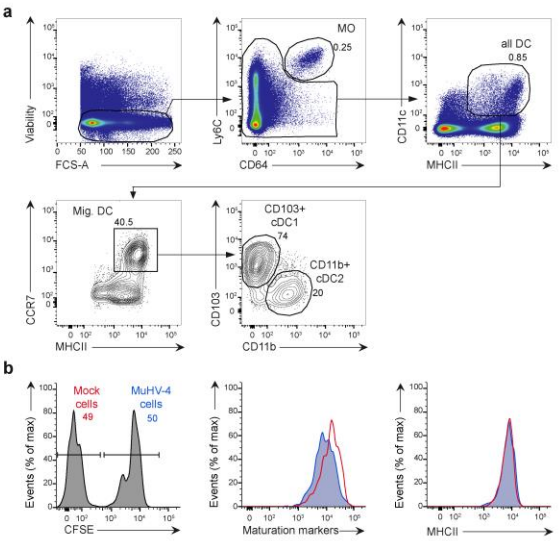

Supplementary Figure 5

Migratory DC subsets in MLNs from mock- and MuHV-4 infected mice after HDM sensitization.

(**a**) Gating strategy for CD103$^+$ cDC1, CD11b$^+$ cDC2, lung-derived CCR7$^+$ DC populations in the MLN of mock or MuHV-4 infected BALB/c mice, HDM sensitized (100 µg) 30 days p.i. and euthanized 2 days later. MLN cells from MuHV-4 infected mice were labelled with CFSE and then mixed with MLN cells from mock-infected mice prior to antibody staining and flow cytometry analysis of a single mix, allowing unbiased comparisons. Debris and doublets were excluded based on FSC and SSC. MOs were excluded based on Ly6c and CD64 expression. Migratory lung-derived CD11b$^+$ cDC2 were identified as liveCD11c$^+$MHC-II^{hi}CCR7$^+$CD11b$^+$ cells. Migratory lung-derived CD103$^+$ cDC1s were identified as liveCD11c$^+$MHC-II^{hi}CCR7$^+$CD103$^+$CD11b^{lo} cells. Representative flow cytometry plots are shown with the mean frequency of the different cells subsets. (**b**) Mean fluorescence intensities of maturation markers (CD40, CD80 and CD86, with independent staining and analysis for each of these markers) and MHCII by migratory DCs subsets were compared between the CFSE$^+$ (originating from MuHV-4 infected mice) and CFSE$^-$ (originating from mock-infected mice) populations. A reciprocal experiment comparing CFSE$^+$ DCs from mock-infected mice to CFSE$^-$ DCs from MuHV-4 infected has been performed as control and gave similar results (not shown).

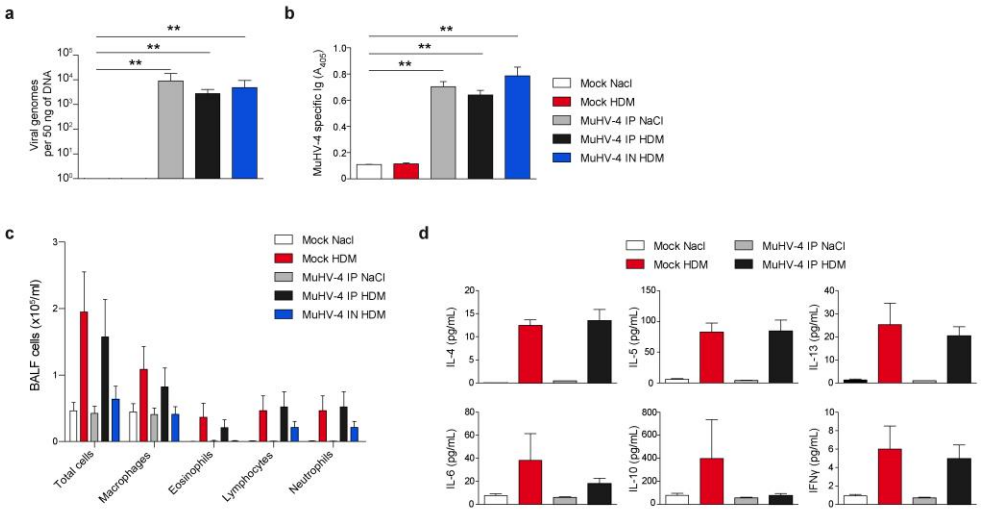

Supplementary Figure 6

Intranasal infection with MuHV-4 protects mice against HDM-induced airway allergy, but intraperitoneal infection does not.

(a-d) Quantification of MuHV-4 genomic copies in splenic cells by qPCR (**a**), quantification of MuHV-4 specific immunoglobulins in sera by ELISA (**b**), total and differential cell counts of BALF cells (**d**), and ELISA measurement of cytokine release by MLN cells following *ex vivo* restimulation by HDM (**d**) at euthanasia of mock, or MuHV-4 infected BALB/c mice either intranasally or intraperitoneally ($1x10^4$ PFU), submitted 30 days p.i. to the HDM-induced high dose model of asthma. ** $p< 0.01$ (Mann-Whitney t-test (**a, b**) or one-way ANOVA and Tukey's multiple comparison test (**c, d**)). Data are representative of 2 independent experiments with 5 mice per group (mean ± s.e.m. in **a-d**).

a

Infection	Treatment	Repeat	Total Reads	No. unique mapped Reads	% mapped	No. reads in UCSC mm10 annotation	% Reads in UCSC mm10 annotation
Mock	Saline	1	34610101	30530928	0,88	29844811	0,86
Mock	Saline	2	40620701	35754355	0,88	35181142	0,87
Mock	Saline	3	35458076	31272761	0,88	30259812	0,85
Mock	HDM	1	37923652	33303891	0,88	32855867	0,87
Mock	HDM	2	40341399	35318424	0,88	34756698	0,86
Mock	HDM	3	42453994	37231156	0,88	36051349	0,85
MuHV-4	Saline	1	39382649	34402028	0,87	34144333	0,87
MuHV-4	Saline	2	21253737	18573858	0,87	17756088	0,84
MuHV-4	Saline	3	36586987	32162111	0,88	31284179	0,86
MuHV-4	HDM	1	35667482	31181425	0,87	30773980	0,86
MuHV-4	HDM	2	34795905	30588071	0,88	30989941	0,89
MuHV-4	HDM	3	36397818	31693843	0,87	31761434	0,87

b

			Mock Saline			Mock HDM			MuHV-4 Saline			MuHV-4 HDM		
Subset marker	Lineage	entrezID	Repl. 1	Repl. 2	Repl. 3	Repl. 1	Repl. 2	Repl. 3	Repl. 1	Repl. 2	Repl. 3	Repl. 1	Repl. 2	Repl. 3
Cd19	B cells	12478,00	0,07	0,03	0,07	0,00	0,03	0,03	0,29	0,34	0,19	0,39	0,26	0,28
Mpo	Neutrophils	17523,00	0,00	0,00	0,00	0,03	0,03	0,00	0,00	0,00	0,00	0,00	0,03	0,00
SiglecS (SiglecF)	Eoinophils/AM	233186,00	428,65	442,34	438,77	226,20	272,41	262,68	179,68	160,45	197,86	129,56	135,66	133,21
Epx	Eosinophils	13861,00	0,00	0,00	0,00	0,03	0,00	0,08	0,00	0,00	0,03	0,00	0,00	0,00
Prg2	Eosinophils	19074,00	0,00	0,00	0,00	0,00	0,03	0,00	0,00	0,00	0,00	0,00	0,00	0,03
Prg3	Eosinophils	53856,00	0,00	0,00	0,00	0,00	0,00	0,00	0,00	0,00	0,00	0,00	0,00	0,00
Lyz2 (LyzM)	Myeloid	17105,00	25464,39	26725,14	26045,27	29460,40	25689,15	27946,28	28315,53	31383,94	28530,33	27664,05	26938,19	29078,85
Emr1 (F4/80)	Macrophage	13733,00	368,00	375,37	389,20	355,67	328,57	338,91	299,00	300,69	306,42	314,91	318,43	330,09
Itgax(Cd11c)	Macrophage	16411,00	2045,28	2060,19	2035,37	3038,79	3025,00	3139,52	1935,58	1958,43	1858,48	2227,82	2364,12	2218,73
Cd3e	T cells	12501,00	0,03	0,00	0,03	1,13	0,83	0,58	5,07	3,77	2,81	24,27	17,13	24,27
Cd3d	T cells	12500,00	0,03	0,06	0,00	0,46	0,20	0,36	1,32	1,18	0,90	15,99	9,10	17,79
Cd3g	T cells	12502,00	0,17	0,09	0,03	0,61	0,69	0,42	4,77	4,56	3,61	23,33	15,94	26,60

*Gene expression levels are RPM normalized == Read count per gene/ (total mapped reads/1000000)

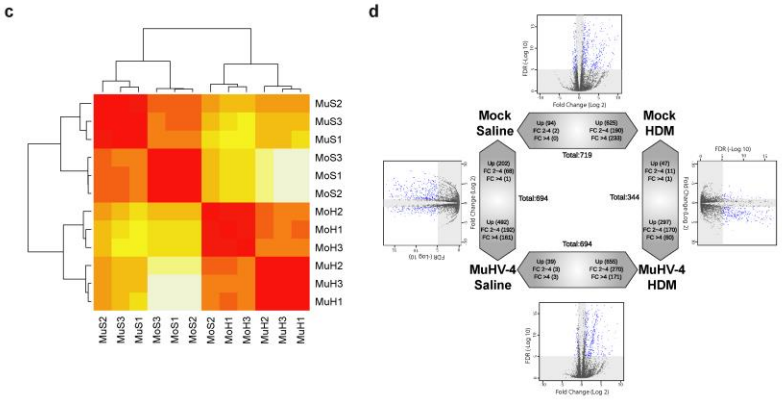

Supplementary Figure 7

Details of the transcriptomics analysis of AMs.

(**a**) Sequence and mapping statistics for raw Illumina data. (**b**) Validation of sample purity by assessing the expression of lineage-restricted marker genes for potential contaminants; eosinophils, neutrophils, B and T cells. (**c**) Unsupervised, hierarchical clustering of individual lanes demonstrating discrete clustering of biologic replicates. (**d**) Summary of differentially expressed (DE) genes (P<1e-5) in each pairwise comparison showing DE genes in blue in volcano plot, showing the total number of DE genes outside the bidirectional arrows, and showing in the arrowheads the direction of upregulated expression for all, moderately (log 2-fold change ± 2-4) and highly (log 2-fold change > 4) DE genes.

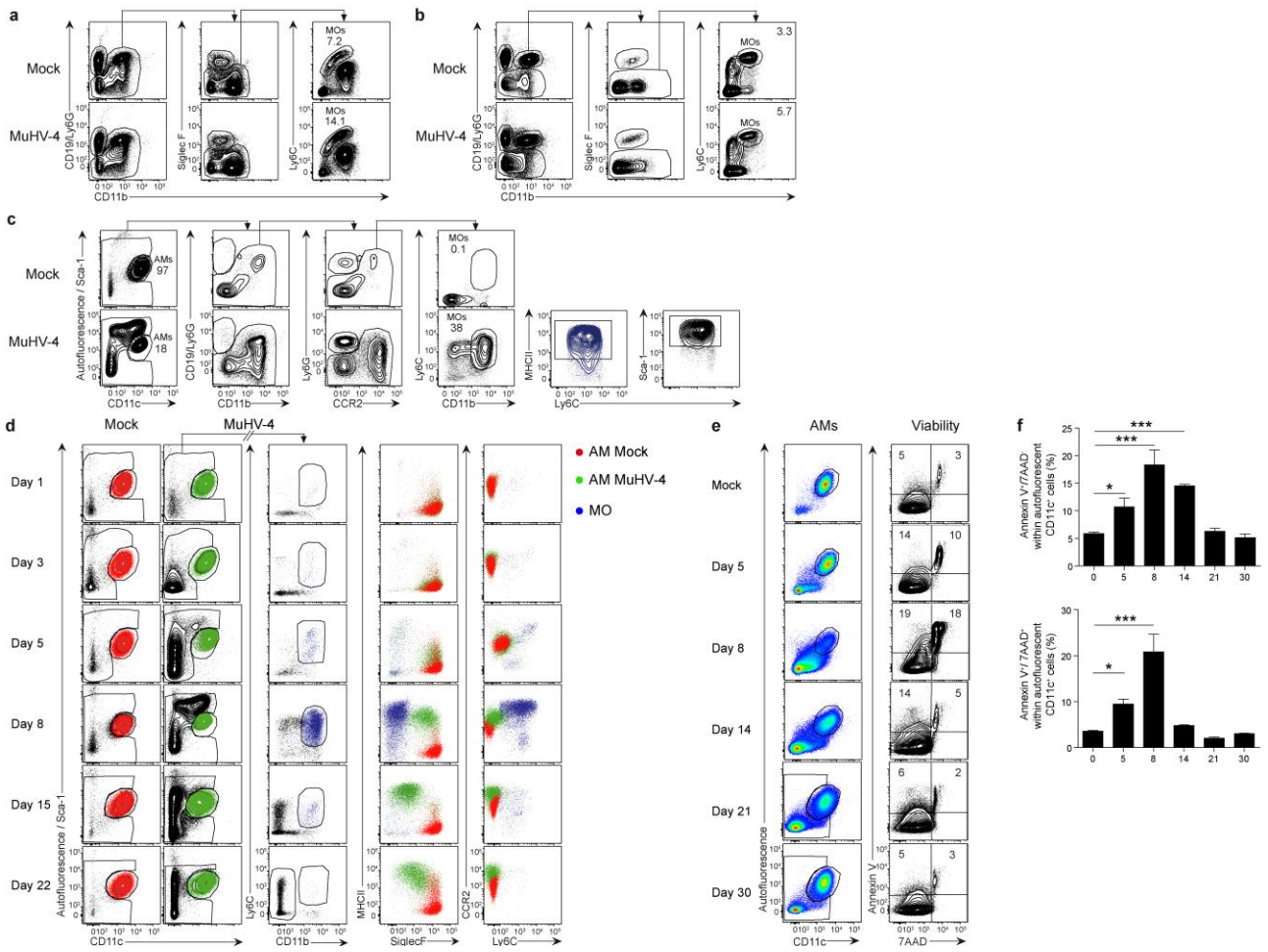

Supplementary Figure 8

Gating strategy for AM and MO subsets in BM, blood and BALF following infection with MuHV-4.

(**a-c**) Flow plots on MO subsets in BM, gated as live$CD19^-CD11b^+SiglecF\text{-}Ly6G^-Ly6C^+$ cells (**a**), on MO subsets in blood gated as live $CD11b^+Ly6G^-CD19^-SiglecF^-Ly6C^+$ cells (**b),** on AM defined as live$autofluorescent^+CD11c^{hi}$ cells (**c**) and BALF MO gated as $nonautofluorescentCD11c^{lo}CD19^-CD11b^+Ly6G^-CCR2^+Ly6C^+$ further analyzed for MHCII and Sca-1 expression (**c**). (**d**) Representative flow cytometry overlays of AM (as defined above) from BALB/c mock-infected mice (red) and AM (green) and MOs (blue) from MuHV-4 infected mice isolated from BALF at the different times p.i.. (**e,f**) Flow cytometry quantification of AM viability in BALF at different times p.i. using Annexin V-APC/7-AAD staining. Representative flow cytometry plots (**e**) and quantification of $Annexin^+/7AAD^-$ and $Annexin^+/7AAD^+$ cells among AM (**f**) from mock or MuHV-4-infected BALB/c mice at different times p.i.. Data are mean ± s.e.m. of samples from 5 mice per group. *** $p< 0.001$, ** $p< 0.01$ and * $p < 0.05$ (in (**f**), all data were compared to values obtained at day 0 by one-way ANOVA and Dunnett's multiple comparison test).

Supplementary Table S1. List of the different clusters of AM genes

Genes		Log2 expression levels												Mock HDM vs MuHV4 HDM p-value
		Mock NaCl1	Mock NaCl2	Mock NaCl3	Mock HDM1	Mock HDM2	Mock HDM3	MuHV-4 NaCl1	MuHV-4 NaCl2	MuHV-4 NaCl3	MuHV-4 HDM1	MuHV-4 HDM2	MuHV-4 HDM3	
M1 orientation	H2-Ea-ps	11,37	11,51	11,37	11,48	11,15	11,05	14,34	13,88	14,12	13,45	13,38	13,48	0,000
	Socs3	9,21	9,29	9,12	11,30	11,76	11,74	10,60	9,94	10,18	11,79	11,69	11,71	0,148
	Socs1	6,01	5,99	5,83	7,98	8,36	7,96	7,23	6,61	6,90	8,65	8,72	8,79	0,000
	H2-L	14,44	14,59	14,40	14,73	14,74	14,64	15,11	14,66	14,98	15,18	15,21	15,20	0,000
	H2-DMa	12,64	12,78	12,60	12,26	12,25	12,25	13,23	12,84	13,16	12,68	12,72	12,73	0,000
	H2-T22	13,04	13,16	12,98	13,55	13,46	13,38	13,76	13,35	13,62	14,02	14,05	14,07	0,000
	Hif1a	11,50	11,70	11,60	11,94	11,90	11,99	11,79	11,70	11,73	12,11	12,01	12,05	0,001
	Cxcl10	7,31	7,38	7,05	11,06	11,19	11,36	7,57	7,63	7,53	11,19	11,31	11,21	0,187
	Ifnb1	1,48	1,48	1,48	1,51	1,52	1,54	1,48	1,50	1,48	1,54	1,65	1,58	0,154
	Ifngr1	12,16	12,36	12,23	11,86	11,90	11,87	12,57	12,21	12,41	12,14	12,03	12,23	0,000
	Il12b	4,75	4,72	4,70	5,71	5,55	5,62	4,72	4,76	4,77	6,16	6,02	6,30	0,000
	Il6	4,04	4,06	4,04	4,64	4,51	4,65	4,04	4,09	4,07	5,12	4,98	4,97	0,000
	Cxcl9	7,45	7,43	7,37	9,34	8,39	8,58	9,60	9,10	9,38	10,14	9,99	9,99	0,000
	Ccl20	0,52	0,52	0,52	0,54	0,52	0,54	0,52	0,53	0,52	0,54	0,54	0,54	0,814
	Ccl22	7,23	7,19	7,17	7,97	8,25	8,20	6,94	6,63	6,95	8,79	8,34	8,59	0,000
	Ccl5	6,36	6,57	6,40	8,43	8,12	8,19	8,22	7,82	7,59	10,83	10,56	10,72	0,000
	Stat1	12,69	12,84	12,73	13,98	13,65	13,74	13,27	13,00	13,20	14,16	14,16	14,16	0,000
	Il27	6,62	6,62	6,57	6,91	6,72	6,74	6,94	6,76	6,93	7,27	7,33	7,33	0,000
	Irf5	11,69	11,81	11,69	12,14	12,33	12,34	12,05	11,75	12,05	12,26	12,23	12,22	0,295
	Cxcl11	5,23	5,25	5,26	7,69	7,60	7,89	5,40	5,56	5,37	8,29	8,53	8,50	0,000
	H2-K2	13,11	13,21	13,03	13,56	13,52	13,44	13,84	13,44	13,73	14,02	14,06	14,06	0,000
M2 orientation	Fabp4	9,12	9,16	9,03	8,56	8,88	8,75	8,62	8,48	8,39	8,20	8,38	8,13	0,000
	Arg1	4,29	4,26	4,39	5,29	5,34	5,39	4,26	4,35	4,32	5,55	4,87	5,22	0,963
	Cd36	12,25	12,47	12,45	12,93	12,87	13,32	11,58	11,19	11,28	12,01	11,93	12,13	0,000
	Chil1	5,58	5,66	5,49	8,39	8,85	8,41	5,33	5,60	5,38	8,05	7,60	7,60	0,000
	Chil3	16,56	16,77	16,67	16,94	16,37	16,93	16,15	16,10	16,33	15,90	16,00	15,99	0,000
	Slc25a1	10,84	11,00	10,81	10,80	10,81	10,71	10,71	10,37	10,60	10,39	10,46	10,47	0,000
	Epas1	9,89	10,01	9,91	10,09	10,27	9,98	9,38	9,13	9,30	9,34	9,31	9,31	0,000
	Erh	10,36	10,53	10,31	10,64	10,48	10,61	10,41	10,09	10,26	10,39	10,40	10,44	0,420
	Il1r1	6,97	6,98	6,92	6,42	6,69	6,63	6,29	6,15	6,30	6,04	6,06	6,11	0,000
	Irf4	9,01	9,00	8,90	9,81	10,05	10,26	9,65	9,57	9,70	9,77	9,67	9,74	0,041
	Mmp9	5,59	5,69	5,52	8,52	9,15	8,79	5,39	5,61	5,66	7,88	7,33	7,38	0,000
	Mrc1	16,30	16,42	16,34	16,07	16,02	16,14	16,20	16,01	16,17	15,77	15,86	15,81	0,001
	Pparg	12,25	12,37	12,26	12,00	12,00	12,05	12,21	11,86	12,17	11,77	11,87	11,82	0,083
	Ppargc1a	0,59	0,59	0,59	0,65	0,59	0,63	0,59	0,60	0,59	0,61	0,59	0,59	0,450
	Stab1	6,53	6,63	6,59	7,68	7,97	7,99	7,64	7,33	7,41	8,79	8,48	8,72	0,000
	Ccl17	5,60	5,56	5,54	7,66	7,90	8,27	5,68	5,61	5,46	6,95	6,37	6,74	0,000
	Clec4a2	11,68	11,93	11,80	12,02	11,87	12,08	11,93	11,71	11,83	11,73	11,71	11,77	0,024
	Ccl24	1,62	1,62	1,62	1,70	1,70	1,70	1,66	1,63	1,68	1,70	1,68	1,66	0,882
	Retnla	1,95	1,95	1,95	2,18	2,06	2,08	1,95	1,96	1,95	1,97	2,08	2,03	0,395
	Cd200r1	11,87	12,10	12,03	12,16	12,00	12,29	12,02	11,91	12,02	11,95	11,99	12,06	0,648
	Chia1	1,73	1,77	1,83	1,79	1,81	1,81	1,71	1,72	1,71	1,71	1,73	1,79	0,425
Mreg orientation	Socs3	9,21	9,29	9,12	11,30	11,76	11,74	10,60	9,94	10,18	11,79	11,69	11,71	0,148
	Il10	1,86	1,86	1,86	1,86	1,88	1,86	1,86	1,87	1,86	2,02	2,02	2,22	0,000
	Il4ra	11,90	12,08	11,86	12,11	12,42	12,23	12,52	12,10	12,50	12,28	12,27	12,30	0,160
	Nfil3	9,84	9,96	9,85	10,00	10,23	10,09	10,29	9,83	10,10	10,21	10,15	10,22	0,012
	Ccl1	0,25	0,25	0,25	0,25	0,25	0,25	0,25	0,26	0,27	0,25	0,25	0,27	0,775
	Ccl22	7,23	7,19	7,17	7,97	8,25	8,20	6,94	6,63	6,95	8,79	8,34	8,59	0,000
	Sphk1	4,31	4,33	4,39	5,05	5,13	5,25	4,41	4,40	4,36	5,66	5,57	5,54	0,000
	Stat3	12,77	12,89	12,74	12,83	12,96	12,91	12,95	12,57	12,87	12,95	12,97	12,93	0,001
	Sbno2	12,61	12,70	12,58	12,86	13,03	12,96	12,79	12,44	12,77	12,92	12,86	12,85	0,801
	Tnfsf14	5,61	5,84	5,63	7,35	7,87	7,83	6,72	6,41	6,56	7,75	7,57	7,60	0,905
	Il27ra	8,47	8,70	8,42	8,66	8,73	8,73	8,92	8,63	8,80	8,90	8,96	8,99	0,000
	Trem2	11,30	11,48	11,29	11,13	11,26	10,95	12,50	11,93	12,25	11,83	11,81	11,91	0,000
	Ly6a	6,36	6,19	6,33	8,41	8,12	8,02	6,52	6,81	6,36	10,23	9,90	10,39	0,000
	Nos2	4,59	4,59	4,56	4,93	5,24	5,00	5,44	5,02	4,91	7,06	7,54	7,50	0,000
	Tnf	9,38	9,49	9,35	10,55	10,90	10,89	9,11	8,90	9,13	10,37	10,30	10,35	0,000
AM surface markers	Emr1	13,41	13,58	13,48	13,47	13,43	13,50	13,33	13,06	13,27	13,28	13,30	13,36	0,335
	Fcgr1	11,56	11,72	11,51	12,10	11,79	11,88	12,29	11,97	12,19	12,62	12,72	12,65	0,000
	Itgax	15,97	16,13	15,98	16,48	16,51	16,59	16,05	15,78	15,92	16,09	16,16	16,12	0,000
	Mertk	12,17	12,28	12,16	12,18	12,16	12,00	12,39	12,14	12,25	12,05	11,93	11,90	0,613
	Siglecf	13,41	13,61	13,45	12,85	13,08	13,08	12,66	12,27	12,66	12,23	12,29	12,29	0,000
AM transcription factors	Hat1	10,32	10,54	10,50	10,88	10,59	10,86	10,14	10,11	10,22	10,48	10,38	10,49	0,024
	Ctnnb1	14,84	15,01	14,91	14,87	15,01	15,02	15,01	14,71	14,92	14,87	14,89	14,90	0,758
	Runx2	10,96	11,11	11,04	10,59	10,78	10,84	10,94	10,65	10,83	10,61	10,57	10,66	0,769
	Cyp27b1	2,23	2,18	2,22	2,16	2,19	2,27	2,18	2,20	2,30	2,18	2,20	2,20	0,913
	Egr2	11,73	11,88	11,74	12,04	12,26	12,29	11,93	11,82	12,09	11,89	11,94	11,88	0,010
	Fosl2	12,75	12,90	12,78	12,58	12,85	12,90	12,81	12,49	12,76	12,51	12,46	12,47	0,001
	Hmgn2	13,10	13,27	13,17	13,18	13,11	13,23	12,91	12,70	12,84	12,78	12,82	12,83	0,000
	Lmo4	12,67	12,81	12,65	12,82	12,87	12,98	12,58	12,21	12,51	12,43	12,49	12,46	0,000
	Lrrfip1	13,96	14,11	13,95	13,73	13,86	13,80	13,92	13,56	13,87	13,60	13,72	13,67	0,686
	Maff	9,44	9,53	9,34	10,11	10,63	10,54	9,34	9,19	9,25	9,92	9,92	9,80	0,000
	Rara	12,13	12,27	12,08	11,60	12,04	11,92	12,17	11,81	12,33	11,81	11,89	11,78	0,717
	Rbl1	11,30	11,46	11,41	11,24	11,25	11,34	11,19	11,03	11,20	11,11	11,06	11,12	0,175
	Baz1a	13,81	13,94	13,86	13,56	13,64	13,59	13,82	13,52	13,72	13,27	13,34	13,31	0,000
	Trerf1	11,52	11,66	11,49	10,91	11,17	10,96	11,54	11,14	11,44	10,83	10,84	10,74	0,156
	Creb5	9,68	9,82	9,81	10,04	10,28	10,45	9,70	9,52	9,71	10,08	10,04	10,09	0,385
	Ncoa4	15,17	15,34	15,26	15,02	15,03	15,02	14,96	14,77	14,89	14,56	14,65	14,63	0,000
	Lsr	11,59	11,73	11,52	10,89	11,01	10,89	11,77	11,32	11,72	10,92	11,07	11,02	0,029
	Lima1	13,33	13,44	13,32	12,63	12,92	12,82	12,91	12,49	12,79	12,16	12,32	12,22	0,000
	Atad2	11,41	11,58	11,52	11,63	11,57	11,78	11,17	11,14	11,30	11,40	11,27	11,36	0,006
	Wrb	9,29	9,50	9,37	9,60	9,46	9,51	9,25	9,06	9,04	9,09	9,13	9,20	0,000
	Wwtr1	9,96	10,09	9,97	9,70	9,86	9,93	8,65	8,28	8,62	8,55	8,60	8,66	0,000
	Bmpr1a	7,23	7,38	7,52	7,52	7,52	7,65	6,45	6,53	6,49	6,71	6,75	6,71	0,000
	Colec12	11,62	11,76	11,70	11,92	11,76	11,99	12,11	11,86	11,99	11,99	11,91	12,09	0,004

Embryonic-derived signature	Lepr	9,83	10,00	9,93	9,26	9,35	9,39	8,31	7,94	8,44	8,19	8,33	8,14	0,000
	Marco	11,21	11,26	11,09	12,20	11,64	11,57	9,30	8,44	9,18	9,69	9,64	9,49	0,000
	Meis1	7,33	7,54	7,39	7,24	7,21	7,42	6,61	6,44	6,59	6,51	6,61	6,53	0,000
	Sema3a	0,54	0,54	0,54	0,52	0,54	0,52	0,54	0,53	0,52	0,52	0,52	0,52	0,840
	Cdc42bpa	9,96	10,14	10,04	10,18	10,21	10,35	9,11	8,88	9,05	9,14	8,98	9,07	0,000
	Erc2	4,60	4,58	4,53	4,42	4,55	4,45	4,03	3,98	4,13	4,13	4,05	4,07	0,000
	Rasef	3,72	3,74	3,83	3,79	3,80	3,98	3,56	3,60	3,64	3,65	3,79	3,64	0,239
	Prickle2	10,07	10,17	10,11	10,16	10,06	10,16	9,54	9,14	9,38	9,56	9,46	9,45	0,000
	Lphn3	10,08	10,19	10,07	9,30	9,62	9,49	8,47	8,10	8,57	8,22	8,19	8,51	0,000
	530059O14R	0,15	0,15	0,15	0,15	0,15	0,15	0,17	0,16	0,15	0,15	0,15	0,15	NA
	Igf2bp2	9,12	9,39	9,21	9,64	9,93	9,84	8,53	8,19	8,55	9,01	9,01	8,87	0,000
	Lrig3	8,68	8,71	8,66	8,08	8,18	8,01	7,50	7,45	7,62	7,40	7,25	7,39	0,000
	Wfdc10	5,38	5,55	5,34	4,89	5,23	4,96	4,80	4,59	4,70	4,58	4,75	4,76	0,007
	Mustn1	2,17	2,07	2,19	2,13	2,07	2,13	2,07	2,09	2,13	2,15	2,17	2,05	0,849
	Fam135a	10,04	10,25	10,27	10,01	9,88	10,19	9,42	9,39	9,39	9,24	9,13	9,29	0,000
	810011O10R	6,26	6,44	6,36	6,40	6,69	7,25	5,78	5,42	5,71	6,05	5,86	5,81	0,000
	Tcaf1	10,86	10,97	10,91	10,78	10,90	10,94	9,96	9,56	9,85	9,90	9,86	9,89	0,000
	Wwtr1	9,96	10,09	9,97	9,70	9,86	9,93	8,65	8,28	8,62	8,55	8,60	8,66	0,000
Monocytic-derived signature	Apbb2	6,64	6,78	6,71	7,58	7,07	7,05	8,81	8,64	8,79	8,55	8,56	8,67	0,000
	C1qb	6,60	6,85	6,67	6,64	6,62	6,66	10,27	9,51	9,83	9,67	9,55	9,72	0,000
	H2-M2	5,32	5,27	5,30	5,44	5,61	5,49	5,65	5,62	5,60	6,30	6,16	6,00	0,000
	Mef2c	7,99	8,16	7,96	8,10	7,99	8,23	9,35	9,16	9,19	8,68	8,75	8,82	0,000
	Ifi205	6,40	6,30	6,27	7,79	7,45	7,68	7,05	6,98	7,02	8,88	9,00	9,02	0,000
	Pyhin1	7,58	7,64	7,62	9,75	9,31	9,75	9,59	9,53	9,61	11,25	11,27	11,34	0,000
	Akt3	10,40	10,58	10,57	10,68	10,48	10,83	10,75	10,61	10,70	10,84	10,86	10,89	0,001
	A530099J19Ri	3,31	3,35	3,39	3,61	3,56	3,62	3,53	3,42	3,44	3,51	3,50	3,56	0,747
	Retnla	1,95	1,95	1,95	2,18	2,06	2,08	1,95	1,96	1,95	1,97	2,08	2,03	0,395
	Plbd1	6,31	6,39	6,25	7,59	8,01	8,00	7,83	7,31	7,42	8,58	8,06	8,45	0,000
	Slamf7	6,24	6,27	6,24	7,56	7,22	7,27	8,59	8,20	8,24	9,40	9,34	9,50	0,000

Genes which are significantly differentially expressed ($p<0.01$) between Mock HDM and MuHV-4 HDM groups are highlighted in function of the group in which expression is higher (red for Mock HDM and green for MuHV-4 HDM)

Supplementary Table S2. List of the different clusters of genes associated with the *antigen presentation pathway* (KEGG_mmu04612)

	Genes	Log2 expression levels												Mock HDM vs MuHV4 HDM p-value
		Mock NaCl1	Mock NaCl2	Mock NaCl3	Mock HDM1	Mock HDM2	Mock HDM3	MuHV-4 NaCl1	MuHV-4 NaCl2	MuHV-4 NaCl3	MuHV-4 HDM1	MuHV-4 HDM2	MuHV-4 HDM3	
Antigen presentation	H2-Ea-ps	11,37	11,51	11,37	11,48	11,15	11,05	14,34	13,88	14,12	13,45	13,38	13,48	0,000
	Gm11127	13,46	13,57	13,40	13,87	13,88	13,75	14,22	13,75	14,06	14,36	14,42	14,40	0,000
	H2-Q6	14,00	14,13	13,93	14,45	14,46	14,32	14,84	14,43	14,74	15,09	15,09	15,12	0,000
	H2-M10.3	1,78	1,76	1,80	1,80	1,81	1,78	1,76	1,80	1,78	1,91	1,89	1,84	0,116
	B2m	15,19	15,37	15,25	15,97	15,73	15,92	15,73	15,52	15,64	16,19	16,15	16,22	0,000
	Ciita	8,48	8,56	8,42	8,43	8,30	7,98	10,89	10,47	10,79	10,14	9,97	9,95	0,000
	Calr	15,29	15,42	15,26	16,01	16,02	16,06	15,43	15,22	15,39	15,73	15,82	15,76	0,000
	Canx	14,20	14,37	14,31	14,61	14,58	14,77	14,32	14,15	14,33	14,42	14,44	14,46	0,066
	Cd4	5,26	5,40	5,35	6,30	6,49	6,32	6,31	6,28	6,29	6,65	6,51	6,88	0,002
	Cd8a	5,55	5,54	5,52	6,71	6,49	6,53	7,83	7,64	7,23	9,87	9,34	9,92	0,000
	Cd8b1	5,33	5,30	5,36	6,22	6,05	5,85	7,23	6,89	6,85	9,41	8,97	9,48	0,000
	Creb1	10,95	11,15	11,14	11,06	11,13	11,37	11,16	11,08	11,20	11,07	10,92	11,08	0,581
	Ctsb	15,99	16,18	16,01	16,69	16,63	16,66	16,30	16,02	16,14	16,63	16,62	16,67	0,125
	Ctsl	13,04	13,22	13,03	13,92	13,86	13,86	13,31	13,03	13,08	13,99	13,99	14,10	0,000
	Ctss	16,99	17,13	17,01	17,16	17,04	17,15	17,63	17,37	17,43	17,48	17,54	17,60	0,000
	Pdia3	14,29	14,45	14,37	15,01	14,86	15,08	14,40	14,31	14,36	14,74	14,74	14,79	0,143
	Hspa5	14,74	14,90	14,75	15,67	15,76	15,89	14,98	14,73	14,94	15,63	15,62	15,64	0,442
	H2-Aa	12,81	12,97	12,80	12,97	12,61	12,55	15,50	15,02	15,27	14,81	14,75	14,77	0,000
	H2-Ab1	12,53	12,69	12,43	12,74	12,52	12,32	15,32	14,69	15,07	14,60	14,63	14,60	0,000
	H2-Bl	12,20	12,31	12,14	12,62	12,65	12,52	12,99	12,52	12,80	13,11	13,21	13,15	0,000
	H2-D1	16,41	16,56	16,35	16,67	16,67	16,60	17,10	16,66	16,95	17,13	17,19	17,17	0,000
	H2-Eb1	12,20	12,33	12,13	12,52	12,33	12,13	15,30	14,70	15,07	14,58	14,62	14,58	0,000
	H2-K1	15,25	15,38	15,19	15,67	15,65	15,59	16,03	15,63	15,92	16,22	16,24	16,25	0,000
	H2-L	14,44	14,59	14,40	14,73	14,74	14,64	15,11	14,66	14,98	15,18	15,21	15,20	0,000
	H2-M10.1	1,14	1,14	1,18	1,16	1,14	1,14	1,16	1,15	1,14	1,16	1,26	1,22	0,090
	H2-M2	5,32	5,27	5,30	5,44	5,61	5,49	5,65	5,62	5,60	6,30	6,16	6,00	0,000
	H2-M3	9,60	9,82	9,65	10,00	9,81	9,84	10,51	10,09	10,34	10,56	10,47	10,63	0,000
	H2-M9	2,04	2,00	2,00	2,04	1,96	2,00	1,98	1,97	2,09	2,00	2,13	2,04	0,419
	H2-DMa	12,64	12,78	12,60	12,26	12,25	12,25	13,23	12,84	13,16	12,68	12,72	12,73	0,000
	H2-DMb1	10,98	11,14	10,98	10,96	10,61	10,57	13,49	12,94	13,25	12,65	12,69	12,71	0,000
	H2-DMb2	11,00	11,16	10,98	10,91	10,57	10,56	13,35	12,85	13,16	12,54	12,53	12,59	0,000
	H2-Oa	4,98	5,12	5,00	5,05	5,12	5,04	5,49	5,36	5,46	5,48	5,41	5,39	0,000
	H2-Ob	3,98	3,89	3,98	4,11	4,19	4,29	4,34	4,24	4,48	4,45	4,26	4,43	0,079
	H2-Q1	13,78	13,91	13,74	14,15	14,19	14,05	14,48	14,05	14,36	14,62	14,66	14,65	0,000
	H2-Q10	13,30	13,42	13,24	13,66	13,63	13,54	13,98	13,62	13,92	14,19	14,21	14,20	0,000
	H2-Q2	12,31	12,47	12,22	12,71	12,74	12,63	13,16	12,67	12,95	13,28	13,37	13,32	0,000
	H2-Q4	14,13	14,25	14,00	14,50	14,54	14,38	14,95	14,47	14,82	15,10	15,13	15,13	0,000
	H2-Q7	13,50	13,63	13,42	13,84	13,89	13,75	14,29	13,88	14,20	14,51	14,50	14,51	0,000
	H2-Q8	14,34	14,49	14,30	14,74	14,78	14,64	15,11	14,71	15,03	15,33	15,33	15,34	0,000
	H2-T10	10,66	10,78	10,56	11,24	11,03	11,04	11,39	10,90	11,21	11,76	11,81	11,82	0,000
	H2-T22	13,04	13,16	12,98	13,55	13,46	13,38	13,76	13,35	13,62	14,02	14,05	14,07	0,000
	H2-T23	13,80	13,90	13,74	14,50	14,35	14,28	14,57	14,13	14,42	14,91	14,96	14,96	0,000
	H2-T24	9,59	9,62	9,51	12,47	12,09	12,29	10,34	10,15	10,37	12,49	12,59	12,55	0,001
	H2-T3	8,01	8,15	7,90	8,36	8,42	8,33	8,69	8,28	8,73	9,02	8,94	8,99	0,000
	H2-T9	13,14	13,26	13,08	13,65	13,55	13,48	13,86	13,44	13,71	14,13	14,16	14,18	0,000
	Hspa8	16,65	16,81	16,65	16,99	17,19	17,32	16,79	16,48	16,74	17,24	17,21	17,32	0,003
	Hspa1l	7,93	7,92	7,64	8,08	8,73	8,83	8,64	8,28	8,00	8,52	8,56	8,66	0,843
	Hspa1b	11,20	11,30	11,02	11,54	12,21	12,38	12,09	11,71	11,42	12,13	12,03	12,15	0,767
	Hspa2	6,94	7,06	6,93	6,75	6,83	6,84	7,13	6,97	7,03	6,97	6,85	6,91	0,083
	Hsp90ab1	15,49	15,62	15,46	15,82	15,92	15,92	15,53	15,26	15,45	15,82	15,86	15,85	0,088
	Hsp90aa1	13,13	13,25	13,19	13,77	13,81	14,05	13,15	13,07	13,09	13,85	13,77	13,81	0,806
	Hspa4	12,79	12,92	12,85	13,08	13,01	13,19	12,83	12,70	12,76	12,82	12,82	12,86	0,007
	Ifng	3,46	3,46	3,46	3,78	3,67	3,59	3,65	3,52	3,55	4,15	4,04	4,19	0,000
	Cd74	14,75	14,88	14,73	14,76	14,59	14,45	17,19	16,72	17,07	16,50	16,56	16,46	0,000
	Klrc1	5,04	5,00	4,98	5,72	5,43	5,58	6,48	6,38	5,99	7,86	7,61	7,96	0,000
	Klrc2	4,41	4,41	4,41	4,67	4,49	4,69	5,23	5,09	5,12	6,42	6,02	6,35	0,000
	Klrd1	4,42	4,45	4,42	5,21	4,71	4,97	5,05	5,02	4,72	5,90	5,50	6,02	0,000
	Rfxap	7,88	7,96	7,88	7,78	7,90	7,80	8,18	7,58	7,95	7,79	7,88	8,02	0,242
	Nfya	11,74	11,88	11,71	11,65	11,81	11,80	11,87	11,69	11,83	11,65	11,66	11,66	0,998
	Nfyb	8,23	8,44	8,30	8,47	8,54	8,64	8,34	8,35	8,35	8,50	8,47	8,48	0,901
	Nfyc	10,46	10,61	10,43	10,31	10,43	10,38	10,55	10,24	10,50	10,21	10,29	10,21	0,558
	Lgmn	13,54	13,70	13,54	13,73	13,72	13,73	14,01	13,68	13,86	13,93	13,97	13,97	0,000
	Psme1	11,95	12,11	11,84	12,71	12,52	12,46	12,31	11,90	12,15	12,74	12,78	12,80	0,000
	Psme2	11,99	12,11	11,93	13,19	12,85	12,86	12,24	11,92	12,14	13,01	13,03	13,09	0,181
	Psme3	11,65	11,81	11,69	11,83	11,83	11,90	11,72	11,43	11,59	11,60	11,66	11,68	0,009
	Hspa1a	11,20	11,30	11,02	11,51	12,15	12,32	12,06	11,70	11,39	12,02	11,92	12,07	0,859
	Rfxank	8,50	8,58	8,44	8,36	8,46	8,31	8,71	8,26	8,56	8,31	8,35	8,43	0,554
	Tap1	10,93	11,06	10,88	12,37	12,11	12,14	11,89	11,51	11,82	12,83	12,71	12,83	0,000
	Tap2	11,51	11,63	11,43	12,15	12,03	11,94	12,05	11,64	11,95	12,47	12,51	12,49	0,000
	Tapbp	13,90	14,04	13,90	15,03	14,77	14,81	14,25	13,88	14,10	14,91	14,93	14,91	0,163
	Tnf	9,38	9,49	9,35	10,55	10,90	10,89	9,11	8,90	9,13	10,37	10,30	10,35	0,000
	H2-M10.4	0,95	0,95	0,95	0,97	0,95	0,95	0,97	0,99	0,95	0,97	1,03	1,01	0,148
	H2-M11	0,35	0,35	0,35	0,35	0,35	0,35	0,37	0,36	0,35	0,35	0,39	0,35	0,613
	H2-M1	0,60	0,60	0,60	0,62	0,60	0,60	0,62	0,61	0,60	0,62	0,60	0,66	0,527
	H2-M10.5	0,69	0,69	0,67	0,69	0,67	0,67	0,67	0,68	0,67	0,67	0,69	0,73	0,534
	H2-M5	4,93	5,25	5,04	5,26	5,54	5,44	5,89	5,24	5,31	5,65	5,67	5,53	0,229
	Kir3dl2	0,29	0,29	0,29	0,29	0,31	0,29	0,29	0,32	0,29	0,29	0,29	0,29	0,822
	Kir3dl1	0,04	0,04	0,04	0,04	0,04	0,04	0,04	0,05	0,04	0,04	0,04	0,04	NA
	H2-M10.2	3,70	3,88	3,78	3,83	3,79	3,79	3,93	3,82	3,85	4,09	3,97	4,05	0,003
	H2-M10.6	1,04	1,06	1,04	1,10	1,04	1,04	1,04	1,05	1,04	1,08	1,14	1,08	0,382
	Rfx5	9,31	9,44	9,27	9,13	9,19	9,19	9,34	9,28	9,39	9,09	9,16	9,07	0,799
	Klrc3	4,33	4,33	4,33	4,63	4,51	4,60	5,17	4,89	4,80	5,99	5,78	5,97	0,000
	Psme2b	10,46	10,51	10,39	11,25	11,01	11,05	10,68	10,31	10,60	11,34	11,31	11,38	0,000
	Gm7030	13,05	13,13	12,96	13,42	13,41	13,26	13,73	13,26	13,58	13,84	13,92	13,88	0,000
	Ifi30	13,48	13,62	13,41	13,71	13,74	13,72	13,55	13,23	13,46	13,57	13,59	13,58	0,480
	C920025E04Rik	12,08	12,25	12,13	12,53	12,54	12,47	12,74	12,39	12,74	13,03	12,96	12,99	0,000
	Gm8909	13,24	13,35	13,16	13,60	13,61	13,48	13,96	13,53	13,87	14,08	14,13	14,12	0,000

Genes which are significantly differentially expressed ($p<0.01$) between Mock HDM and MuHV-4 HDM groups are highlighted in function of the group in which expression is higher (red for Mock HDM and green for MuHV-4 HDM)